JOINT INSTITUTE FOR AERONAUTICS AND ACOUSTICS

National Aeronautics and Space Administration
Ames Research Center

JIAA TR - 69

Stanford University

THE AERODYNAMICS OF DELTA WINGS OF ELLIPTICAL CROSS-SECTION WITH SEPARATED FLOW

BY

Nikos J. Mourtos and Domingo A. Tavella

Stanford University
Department of Aeronautics and Astronautics
Stanford, CA 94305

DECEMBER 1985

ACKNOWLEDGEMENT

The author would like to express his appreciation to professor and director of the Joint Institute, L. Roberts for his ideas, encouragement and valuable suggestions during the course of this research.

ABSTRACT

The "single line vortex with a straight feeding vortex sheet" model has been used to model the steady, inviscid, incompressible, conical flow field around a delta wing with elliptical cross-section exhibiting leading-edge separation. The effect of the location of the separation points on the formation of the vortices, on their strength and position, as well as on the resulting lift on the wing has also been studied.

The results show that :

(i) A delta wing with elliptical cross-section has a higher lift curve slope than a flat delta wing.

(ii) Significant gain in lift can be realized by forcing the separation points away from their natural positions on the upper surface of the wing, towards the leading-edge or even farther on the wing's lower surface.

(iii) Both of the advantages mentioned above cannot be realized at small angles of attack, due to the increased difficulty in the formation of the vortex system as the wing becomes thicker and/or the separation points are moved away from their natural positions.

NOMENCLATURE

English letter symbols :

a	semi-major axis of the elliptical cross-section of the wing
a_0	term in w_s defined in appendix 1
b	semi-minor axis of the elliptical cross-section of the wing
b_0	term in w_s defined in appendix 1
c	$= \sqrt{a^2 - b^2}$, geometric parameter of the ellipse
C_L	lift coefficient
C_p	pressure coefficient
$\Im$	denotes the imaginary part of the complex quantity involved
k	$= \Gamma/2\pi$, vortex strength
L	lift force
N	normal force
p	static pressure
q	dynamic pressure
R	$= (a+b)/2$, local radius of the transformed circular cone
$\Re$	denotes the real part of the complex quantity involved
s	SP location in the physical cross-flow plane (σ-plane)
S	area of the cross-section of the wing
S_{wp}	projected wing area
t	SP location in the transformed cross-flow plane (θ-plane)
u	cross-flow velocity component along the y-axis
U	velocity component along the x-axis
v	cross-flow velocity component along the z-axis
V	transformed velocity defined by equation (31)
V_n	fluid velocity normal to the line vortex
w	complex potential
w_s	complex potential due to a line source distribution
w_{s1}, w_{s2}	components of w_s defined by equations (7) and (8) respectively
W	velocity component along the z-axis
x, y, z	cartesian coordinates fixed at the apex of the wing

Greek letter symbols :

α	angle of attack
β	$= \sqrt{1 - M_\infty^2}$
γ	vortex sheet strength
Γ	circulation of the line vortex
δ	wing semi-apex angle in the (x, z) plane
δ_y, δ_z	excursions of the SP from the LE along the y and z axes respectively
ε	wing semi-apex angle in the (x, y) plane
ς	complex variable in the vertical flat-plate plane
η	distance of the SP from the LE along the surface of the ellipse
θ	complex variable in the circle plane
ξ	dummy variable used for integration in appendix 1
ρ	fluid density
σ	complex variable in the ellipse plane
φ	perturbation velocity potential
Φ	total velocity potential
ψ	perturbation stream function

Subscripts :

cf	refers to the cross-flow plane
x, y, z	denote partial derivatives with respect to x,y,z respectively
∞	refers to the undisturbed flow field
1	refers to the vortex position

Superscripts :

$\bar{}$	denotes the complex conjugate of the parameter involved

Abbreviations :

LE	leading edge
SP	separation point
SPUS	the separation point is on the upper surface
SPLS	the separation point is on the lower surface

TABLE OF CONTENTS

LIST OF FIGURES

1. INTRODUCTION

It is well known that starting at moderate angles of attack, the flow separates from the lee side of lifting bodies. From this separation, fluid with high vorticity is convected upwards, away from the wing surface, so that the resulting flow pattern is quite different from that of attached flow in which the vorticity is only appreciable in the boundary layer.

For highly swept-back delta wings, usually a single shear layer arises along the whole length of each leading-edge and rolls up into a spiral trailing vortex. The influence of these vortices is so strong, that slender body theory alone is inadequate to accurately estimate the lift on such wings.

A first simlification in an effort to study a complicated flow field such as the one described above, would be to consider an inviscid model of the flow in which the shear layer and the vortex are represented by a spiral vortex sheet embedded in an otherwise irrotational flow. This model has already been studied by Smith (reference 3). To avoid the complexities of a curved vortex sheet, this model can be simplified even further by assuming a straight feeding vortex sheet and a single line vortex.

The second simplification will be to consider the flow to be conical, which implies that all physical properties (such as velocity, pressure etc) are constant along the whole length of any half line originating at the apex of the wing. Although the only strictly conical flows are supersonic, observation suggests that the flow over the former half of a slender delta wing is nearly conical and therefore the assumption of conicality is a reasonable one.

Since leading-edge separation is essentially confined to highly swept wings, the application of slender body theory to the single line vortex model seems appropriate. In addition, the use of the slender body theory avoids the difficulty associated with the assumption of a subsonic, conical flow (references 2,3).

Thus, the free stream can be either subsonic or supersonic, but in the later case both the cross-flow velocity component as well as the velocity component normal to the leading-edge must be subsonic.

The main purpose of this work is to obtain a fast estimate of the velocity and pressure fields in the neighborhood of the leading edge, which can then be used in pursuing an analysis of the boundary layer. This analysis in turn, will enable us to predict the separation point by matching the viscous (inside the boundary layer) and inviscid (outside the boundary layer) flow fields around the wing.

In addition, the effect of the position of the separation points on the formation of the vortices, on their strength and position, as well as on the resulting lift on the wing, has been studied.

Although the single line vortex model has already been applied on flat delta wings (reference 2), as well as on circular cones (reference 4), and has given us important information about this type of flow, it is necessary to fill the gap in the knowledge of aerodynamics of shapes intermediate between bodies of revolution and flat triangular wings for the following reasons :

First, for all practical purposes wings have to have some thickness in order to house the structure as well as the fuel. Secondly, as Jorgensen has pointed out (reference 5) there are distinct aerodynamic advantages to the use of elliptic cones. With their major axis horizontal, they develop greater lift and have higher lift-to-drag ratios than circular cones of the same fineness ratio and volume.

Last but not least, the geometry of elliptic cones is still sufficiently easy, to make a fairly simple analysis possible.

The geometric characteristics of a delta wing with elliptical cross-section are depicted in figure (1).

2. ANALYSIS OF THE FLOW FIELD

The problem considered here is that of potential flow about a slender delta wing with elliptical cross-section, on which the flow is separated from the leading edge. The equation of motion to be satisfied is :

$$\beta^2 \varphi_{xx} + \varphi_{yy} + \varphi_{zz} = 0 \tag{1}$$

However, if the analysis is restricted to highly swept wings, the first term may be neglected and the equation of motion becomes Laplace's equation for incompressible two-dimensional flow:

$$\varphi_{yy} + \varphi_{zz} = 0 \tag{2}$$

which is valid in the cross-plane (y, z) at any station x along the wing. Thus, the three dimensionality of the problem will enter only through the boundary conditions. Solutions will be sought first for the flow about a circular cone and then transformed by means of conformal mapping to elliptical cones.

2.1 The Complex Potential

Refering to figure (2b), the complex potential for the cross-flow in the transformed (circle) plane is given by :

$$w_{cf}(\theta) = -\imath U_\infty \alpha \left(\theta - \frac{R^2}{\theta}\right) - \imath k \ln \left(\frac{(\theta - \theta_1)}{(\theta + \bar{\theta}_1)} \frac{(\theta\theta_1 + R^2)}{(\theta\bar{\theta}_1 - R^2)}\right) \tag{3}$$

where the first term represents uniform flow past the circle (the angle of attack has been assumed small) and the second term represents a vortex pair in the leeward side together with its image inside the circle (as given by the circle theorem). The Joukowski transformation :

$$\theta = \frac{1}{2}(\sigma + \sqrt{\sigma^2 - c^2}\,) \tag{4}$$

can now be used to express the complex potential for the cross-flow in the physical (ellipse) plane :

$$w_{cf}(\sigma) = -\imath k \ln \frac{(\sigma - \sigma_1 + \sqrt{\sigma^2 - c^2} - \sqrt{\sigma_1^2 - c^2}\,)[(\sigma + \sqrt{\sigma^2 - c^2}\,)(\sigma_1 + \sqrt{\sigma_1^2 - c^2}\,) + 4R^2]}{(\sigma + \bar{\sigma}_1 + \sqrt{\sigma^2 - c^2} + \sqrt{\bar{\sigma}_1^2 - c^2}\,)[(\sigma + \sqrt{\sigma^2 - c^2}\,)(\bar{\sigma}_1 + \sqrt{\bar{\sigma}_1^2 - c^2}\,) - 4R^2]}$$

$$- \frac{\imath}{2} U_\infty \alpha \frac{(\sigma + \sqrt{\sigma^2 - c^2}\,)^2 - 4R^2}{\sigma + \sqrt{\sigma^2 - c^2}}. \tag{5}$$

To this we need to add the complex potential for an expanding ellipse of constant axis ratio, in order to satisfy the tangency condition on the surface of the cone :

$$w_s = w_{s1} + w_{s2} \tag{6}$$

where

$$w_{s1} = U_\infty b\varepsilon \ln \frac{\sigma + \sqrt{\sigma^2 - c^2}}{2} \tag{7}$$

and

$$w_{s2} = -U_\infty \varepsilon \delta \left\{ x \left[\ln 2\sqrt{x(1-x)} - 1 \right] + \frac{1}{2} \right\} \tag{8}$$

The derivation of w_{s1} and w_{s2} is shown in appendix 1. The total complex potential in the physical plane is of course :

$$w = w_{cf} + w_s \tag{9}$$

2.2 The Velocity Field

If the velocity potential Φ is split in two parts :

$$\Phi = U_\infty x + \varphi \tag{10}$$

where

$$\varphi = \Re\{w\} \tag{11}$$

then the components of the velocity at any point are:

$$\Phi_x = U_\infty + \varphi_x \tag{12}$$

where

$$\varphi_x = \Re\left\{\frac{dw}{da}\frac{da}{dx}\right\} = \varepsilon\Re\left\{\frac{dw}{da}\right\} \tag{13}$$

and

$$\Phi_y = \varphi_y = \Re\left\{\frac{dw}{d\sigma}\right\} = \Re\left\{\frac{dw}{d\theta}\frac{d\theta}{d\sigma}\right\} \tag{14}$$

$$\Phi_z = \varphi_z = -\Im\left\{\frac{dw}{d\sigma}\right\} = -\Im\left\{\frac{dw}{d\theta}\frac{d\theta}{d\sigma}\right\} \tag{15}$$

The evaluation of the derivative dw/da is shown in appendix 3.

3. CONDITIONS

The conditions that the solutions of equation (2) must satisfy are the following :

(i) Tangency condition on the wing. This is automatically satisfied by the complex potential of equation (9).

(ii) Separation condition on the wing. The separation point has to be specified since the present inviscid model is unable to predict it.

(iii) The disturbances must vanish at infinity. This condition is also automatically satisfied by the complex potential.

(iv) The fluid pressure must be continuous everywhere. This condition however, cannot be met with the present model. The reason is that for conical flow the strength of the concentrated vortices is increasing linearly in the downstream direction, requiring thus a vortex sheet to connect them with the separation points on the wing, and feed them continuously with vorticity. This difficulty could of course be circumvented by assuming a curved feeding sheet, which would form part of a three-dimensional stream surface. The solution then would provide both the shape and the strength of the sheet (reference 3). However, the problem is greatly simplified by assuming a straight feeding sheet (as in figure 3) and past experience has shown that such a model does capture the main features of the flow. The last condition needs therefore to be replaced by:

(iv)' The vortex system (feeding sheet and concentrated vortex) must be force free.

3.1 Separation Condition

The separation point must also be a stagnation point of the flow. Assuming only small

excursions of the separation point from the leading edge of the wing, its position in the physical plane can be represented by $s(a-\delta_y, \delta_z)$, where δ_y and δ_z are small compared to a. Under the Joukowski transformation s goes into a point t in the θ-plane, given by :

$$t = \frac{1}{2}\left[a - \delta_y + i\delta_z + \sqrt{(a-\delta_y)^2 + 2\delta_z(a-\delta_y)i - \delta_z^2 - c^2}\right] \tag{16}$$

where δ_y and δ_z are related by :

$$\frac{(a-\delta_y)^2}{a^2} + \frac{\delta_z^2}{b^2} = 1 \tag{17}$$

since s is a point of the elliptical cross-section. Solving for δ_z we get :

$$\delta_z = \pm\sqrt{b^2 - \frac{b^2}{a^2}(a-\delta_y)^2} \tag{17a}$$

where the "plus" sign is used when the separation point is on the upper surface and the "minus" sign is used when the separation point is on the lower surface. Requiring the presence of a stagnation point at s is equivalent to :

$$\left.\frac{dw_{cf}}{d\theta}\right]_{\theta=t} = 0 \tag{18}$$

or from equation (3)

$$\frac{U_\infty \alpha}{k} = \left[\frac{\bar{\theta}_1^2 + 2t\bar{\theta}_1 - R^2}{(t+\bar{\theta}_1)(t\bar{\theta}_1 - R^2)} - \frac{R^2 + 2t\theta_1 - \theta_1^2}{(t-\theta_1)(t\theta_1 + R^2)}\right]\frac{t^2}{t^2+R^2} \tag{19}$$

and substituting θ from equation (4) we get :

$$\frac{U_\infty \alpha}{k} = \left\{ \frac{(\bar{\sigma}_1 + \sqrt{\bar{\sigma}_1^2 - c^2})^2 + 4t(\bar{\sigma}_1 + \sqrt{\bar{\sigma}_1^2 - c^2}) - 4R^2}{(2t + \bar{\sigma}_1 + \sqrt{\bar{\sigma}_1^2 - c^2})[t(\bar{\sigma}_1 + \sqrt{\bar{\sigma}_1^2 - c^2}) - 2R^2]} \right.$$

$$\left. + \frac{(\sigma_1 + \sqrt{\sigma_1^2 - c^2})^2 - 4t(\sigma_1 + \sqrt{\sigma_1^2 - c^2}) - 4R^2}{(2t - \sigma_1 - \sqrt{\sigma_1^2 - c^2})[t(\sigma_1 + \sqrt{\sigma_1^2 - c^2}) + 2R^2]} \right\} \frac{t^2}{t^2 + R^2} \tag{20}$$

3.2 Force Balance for the Vortex System

Refering to figure (3), the vector force on each filament representing the vorticity lying between x and $x + dx$ is :

$$\imath\rho U_\infty \frac{d\Gamma}{dx}[\sigma_1 - (a - \delta_y + \imath\delta_z)] \simeq \imath\rho U_\infty \gamma(\sigma_1 - a + \delta_y - \imath\delta_z)$$

where

$$\gamma = \frac{d\Gamma}{dx} = const \tag{21}$$

while the vector force on the concentrated vortex is :

$$-\imath\rho V_n \Gamma = -\imath\rho V_n \gamma \frac{a}{\varepsilon}$$

since

$$\varepsilon \simeq \frac{a}{x} \tag{22}$$

and

$$\Gamma = \gamma x \tag{23}$$

The vector sum of the two forces must be zero :

$$\imath\rho U_\infty \gamma(\sigma_1 - a + \delta_y - \imath\delta_z) - \imath\rho V_n \gamma \frac{a}{\varepsilon} = 0 \Rightarrow$$

$$V_n = U_\infty \varepsilon \frac{\sigma_1 - a + \delta_y - \imath\delta_z}{a} \tag{24}$$

V_n is the sum of the component of the main stream which is normal to the vortex, plus the normal component of the velocity due to the disturbance potential φ. Thus :

$$V_n = -U_\infty \varepsilon \frac{\sigma_1}{a} + [u + \imath v]_{\sigma=\sigma_1} \tag{25}$$

Combining equations (24) and (25) we get :

$$[u + \imath v]_{\sigma=\sigma_1} = U_\infty \varepsilon \left(\frac{2\sigma_1}{a} + \frac{\delta_y - \imath\delta_z}{a} - 1 \right) \tag{26}$$

and after rearranging real and imaginary parts, equation (26) yields :

$$[u - \imath v]_{\sigma=\sigma_1} = U_\infty \varepsilon \left(\frac{2\bar{\sigma}_1}{a} + \frac{\delta_y + \imath\delta_z}{a} - 1 \right) \tag{27}$$

The left hand side of equation (27) represents the mean velocity at the vortex location. To find another expression for it, we need to consider the effect of the total complex potential $w(\sigma)$, less the complex potential of the right-hand vortex, i.e.

$$w_1(\sigma) = w(\sigma) + \imath k \ln(\sigma - \sigma_1) \tag{28}$$

Differentiating to get the velocity :

$$\frac{dw_1}{d\sigma} = \frac{dw}{d\sigma} + \frac{\imath k}{\sigma - \sigma_1} \tag{29}$$

and substituting w from equation (9) while letting $\sigma \to \sigma_1$ finally gives :

$$\begin{aligned}
[u - \imath v]_{\sigma=\sigma_1} = -\imath U_\infty \alpha \left(1 + \frac{\sigma_1}{\sqrt{\sigma_1^2 - c^2}}\right) \left[\frac{1}{2} + \frac{2R^2}{(\sigma_1 + \sqrt{\sigma_1^2 - c^2}\,)^2}\right] \\
+ U_\infty \frac{b\varepsilon}{\sqrt{\sigma_1^2 - c^2}} + \frac{\imath k c^2}{2(\sigma_1^2 - c^2)(\sigma_1 + \sqrt{\sigma_1^2 - c^2}\,)} \\
- \imath k \left(1 + \frac{\sigma_1}{\sqrt{\sigma_1^2 - c^2}}\right) \left[\frac{\sigma_1 + \sqrt{\sigma_1^2 - c^2}}{(\sigma_1 + \sqrt{\sigma_1^2 - c^2}\,)^2 + 4R^2}\right. \\
- \frac{\bar{\sigma}_1 + \sqrt{\bar{\sigma}_1^2 - c^2}}{(\sigma_1 + \sqrt{\sigma_1^2 - c^2}\,)(\bar{\sigma}_1 + \sqrt{\bar{\sigma}_1^2 - c^2}\,) - 4R^2} \\
\left. - \frac{1}{\sigma_1 + \bar{\sigma}_1 + \sqrt{\sigma_1^2 - c^2} + \sqrt{\bar{\sigma}_1^2 - c^2}}\right]
\end{aligned} \tag{30}$$

Comparing equations (27) and (30) while substituting $U_\infty \alpha / k$ from equation (20) yields an equation in one unknown (σ_1) which is solved numerically (see appendix 4) and the results are shown in the next section.

4. RESULTS

4.1 Uniqueness of the solution

Given the thickness of the wing and the position of the separation point, three solutions for the position of the vortex were found (see figure 4) :

In the first solution, the vortex moves farther from the wing and becomes stronger as the angle of attack increases.

In the second solution, which as appears in figure (4) is an extension of the first one, the vortex moves closer to the wing surface and its strength increases as the angle of attack increases.

In the third solution, the vortex is under the wing and again moves farther away and becomes stronger as the angle of attack increases.

The second solution dissappears when the separation point is exactly at the leading edge. It should also be noted that all three families of solutions exist for the limiting cases of the flat triangular wing and the circular cone.

Although it may be interesting to investigate further the posibility of existence as well as the stability of the second and third solutions, they will not be considered further in this report.

4.2 Existence of the Solution

As is shown in figure (4) there is a minimum value of the parameter α/ε below which no solution exists. This is in agreement with experimental observations (see references

5,8,9,10), the explanation being that at small angles of attack the body radius as it grows in the x-direction prevents the departure of free vortices. When the angle of attack becomes sufficiently high, the vorticity in the boundary layer accumulates along rays near the upper surface of the body. The vortices generally do not separate from the body until some higher angle of attack is reached (reference 9).

However, since in this model no account of the viscosity has been taken, this result shows that it is also the kinematics of the flow field which prevents the formation of the vortices at low angles of attack.

In figure (5), the minimum value of α/ε has been plotted against the position of the separation point for wings of various thickness. It can be seen that $(\alpha/\varepsilon)_{min}$ becomes smaller as the thickness of the wing diminishes. In the limiting case of a flat delta wing separation begins immediately for any $\alpha > 0$ (provided that the separation point is fixed at the leading edge). This is also in agreement with experimental observations (references 5,9).

On the other hand, it becomes progressively more difficult to obtain a solution as the separation point is moved from the upper surface towards the leading edge and on the lower surface.

Although no experiments that show the effect of the position of the separation points on the formation of the vortices have been performed yet, intuitively it can be said that since the observed separation point on delta wings with elliptical cross-section is on the upper surface, it is normal to expect some difficulty in the formation of the vortices when the separation point is forced away from its natural position.

4.3 Velocity Distribution on the Upper Surface of the Wing

The conical inviscid solution of the velocity field is a function of y/x rays. Therefore,

it is convenient to transform the velocity in the following way :

$$V = \frac{1}{\varepsilon}\left(\Phi_y - \frac{y}{x}\Phi_x\right) = \frac{1}{\varepsilon}\Phi_y - \frac{y}{a}\Phi_x \tag{31}$$

Plots of this transformed velocity on the upper surface of an elliptical cone with $\varepsilon = 15°$ and $b = 0.2$ exhibiting separation from the leading edge ($\delta_y = 0$), are shown in figure (6) for various angles of attack.

The location of the reattachment line is also shown in these plots and it can be seen that it moves towards the center line of the wing as the angle of attack increases. For this particular wing the two lines finally coincide at $\alpha \simeq 23°$.

At the center line $y = 0$, $dV/dy > 0$ whereas at the reattachment line $dV/dy < 0$. When the two lines coincide then $dV/dy > 0$ as it can be seen in figure (6c).

4.4 Pressure Distribution on the Wing

The velocity field on the surface of the wing can be found by substituting $\sigma = y + iz$ and $z = \pm b\sqrt{1-y^2}$ into equations (13),(14) and (15) while letting y/a vary between -1 and +1. The "plus" sign in z corresponds to points on the upper surface while the "minus" sign corresponds to points on the lower surface. Then, the pressure distribution on the surface of the wing can be found from Bernoulli's equation :

$$p + \frac{1}{2}\rho(\Phi_x^2 + \Phi_y^2 + \Phi_z^2) = p_\infty + \frac{1}{2}\rho(U_\infty^2 + W_\infty^2) = p_\infty + \frac{1}{2}\rho U_\infty^2(1+\alpha^2)$$

since for small α : $\tan\alpha \simeq \alpha$. Now :

$$C_p \equiv \frac{p - p_\infty}{\frac{1}{2}\rho(U_\infty^2 + W_\infty^2)} \simeq 1 + \alpha^2 - \frac{\Phi_x^2 + \Phi_y^2 + \Phi_z^2}{U_\infty^2} \tag{32}$$

but

$$\Phi_x^2 = U_\infty^2 + \varphi_x^2 + 2\varphi_x U_\infty$$

and if $\varepsilon \sim \alpha$ then $\phi_x \sim \alpha^2$ so if only terms of order α^2 are maintained :

$$C_p \simeq \alpha^2 - 2\frac{\varphi_x}{U_\infty} - \frac{\varphi_y^2 + \varphi_z^2}{U_\infty^2} \tag{33}$$

Pressure distributions for a flat triangular wing as well as for two elliptical ones 10 per cent and 20 per cent thick, are shown in figure (7) for three angles of attack (7.5°, 15° and 30°). The separation point has been fixed at the leading edge while the semi-apex angle of the cone has been kept constant $\varepsilon = 15°$ for easy comparison. Several observations can be made from these plots :

(i) The very low pressure region on the upper surface of the wing is caused by the presence of the vortex and the negative pressure peak corresponds approximately to the lateral position of the vortex.

(ii) The negative pressure peak on the upper surface becomes wider and its absolute value increases as the angle of attack increases. This is a result of an increase in the strength of the vortex which thus influences a wider area over the wing.

(iii) Increasing the thickness of the wing also makes the vortex stronger (for the same angle of attack) as can be seen by comparing the negative pressure peak for the three different wings.

(iv) The pressure jump at the leading edge ($y/a = 1$) is of course due to the connecting vortex sheet and it moves around with the separation point.

4.5 Lift

The normal force can be obtained by calculating the change in downward momentum through an infinite plane perpendicular to the longitudinal axis x of the wing at the trailing edge. Thus :

$$N = -\rho U_\infty \iint (\varphi_z - U_\infty \alpha) dz dy \tag{34}$$

Note that φ_z is the velocity component in a plane perpendicular to the wing surface and therefore it contains the upwash contribution of the free stream. Integrating with respect to z produces a contour integral of the velocity potential :

$$N = -\rho U_\infty \int_c \varphi dy \tag{35}$$

The contour c is shown in figure (8a) and includes the wing trace plus the cuts connecting the separation points with the centers of the vortices. The vortices may be included in the body without affecting the normal force since the forces on them cancel those on their feeding sheets.

In terms of the complex potential $w(\sigma) = \varphi + i\psi$, equation (35) can be written as :

$$N = -\rho U_\infty \Re \left\{ \int_c w d\sigma + \int_c \psi dz \right\} \tag{36}$$

but since $\psi = 0$ on the body and is single valued on the vortices and the feeding sheets, the second integral vanishes. Furthermore, the function $w(\sigma)$ is analytic in the field external to the contour; hence, the integral is independent of the path provided that it encloses the original contour. The simplest way to integrate equation (36) is by transforming it to the ς-plane (see figures 2d and 8b) :

$$N = -\rho U_\infty \Re \left\{ \int_c w(\varsigma) \frac{d\sigma}{d\varsigma} d\varsigma \right\} \tag{37}$$

Substituting $\sigma(\varsigma)$ from figure (2) into equation (5) and noting that :

$$\frac{d\sigma}{d\varsigma} = \frac{(\varsigma + \sqrt{\varsigma^2 + 4R^2}\,)^2 - c^2}{2\sqrt{\varsigma^2 + 4R^2}(\varsigma + \sqrt{\varsigma^2 + 4R^2}\,)} \tag{38}$$

equation (37) becomes :

$$N = \rho U_\infty \Re \left\{ i \int_c \left(\frac{\Gamma}{2\pi} \ln \frac{\varsigma - \varsigma_1}{\varsigma + \bar{\varsigma}_1} + U_\infty \alpha \varsigma \right) \frac{(\varsigma + \sqrt{\varsigma^2 + 4R^2}\,)^2 - c^2}{2\sqrt{\varsigma^2 + 4R^2}(\varsigma + \sqrt{\varsigma^2 + 4R^2}\,)} d\varsigma \right\} \tag{39}$$

Note that the source term has been omitted from the complex potential since it is axisymmetric and therefore produces no net downward momentum. The integral of the logarithm can be evaluated by surrounding the contour by a large circle whose radius $\rightarrow \infty$. Since there are no singularities between the contour and the large circle the integrals are equal. The remaining integration is evaluated along the vertical line between the branch points at $\pm i(a+b)$ giving finally :

$$N = \rho U_\infty \Gamma(\varsigma_1 + \bar{\varsigma}_1) + 2\rho U_\infty^2 \pi \alpha \left(R^2 + \frac{c^2}{4} \right) - \rho U_\infty^2 \pi \alpha \left(R - \frac{c^2}{4R} \right) \left(R + \frac{c^2}{4R} \right) \tag{40}$$

Transforming back to the σ-plane gives the result :

$$N = \rho U_\infty \Gamma \Re \left\{ \left(1 + \frac{a+b}{a-b} \right) \sqrt{\sigma_1^2 - c^2} + \left(1 - \frac{a+b}{a-b} \right) \sigma_1 \right\} + \pi \rho U_\infty^2 a^2 \alpha \qquad (41)$$

For small angles of attack (as it has been assumed so far) the normal force can be taken equal to the lift. This is in agreement with the well known result that for a lightly loaded wing (small perturbation flow) the induced drag is a second order quantity.

Defining the lift coefficient as :

$$C_L \equiv \frac{L}{q_\infty S_{wp}} \qquad (42)$$

where

$$q_\infty = \frac{1}{2} \rho U_\infty^2 \qquad (43)$$

and

$$S_{wp} = \frac{1}{2}(2a)x = a\frac{a}{\varepsilon} = \frac{a^2}{\varepsilon} \qquad (44)$$

we get :

$$C_L = \frac{2\Gamma\varepsilon}{U_\infty a^2} \Re \left\{ \left(1 + \frac{a+b}{a-b} \right) \sqrt{\sigma_1^2 - c^2} + \left(1 - \frac{a+b}{a-b} \right) \sigma_1 \right\} + 2\pi\alpha\varepsilon \qquad (45)$$

The second term is the slender body theory result (R.T.Jones), while the first term is the nonlinear contribution of the vortex separation.

Equation (45) can also be written as :

$$\frac{C_L}{\varepsilon^2} = \frac{2\Gamma(\alpha/\varepsilon)}{U_\infty a^2 \alpha} \Re \left\{ \left(1 + \frac{a+b}{a-b}\right) \sqrt{\sigma_1^2 - c^2} + \left(1 - \frac{a+b}{a-b}\right) \sigma_1 \right\} + 2\pi \frac{\alpha}{\varepsilon} \qquad (46)$$

Figure (9) shows how the lift coefficient varies with angle of attack for different positions of the separation point. A comparison of figures (9a) (flat plate) and (9b) (ellipse 10 per cent thick), shows that the general trend is to get higher C_L as thickness is added on the wing. It can also be seen that for a given thickness of the wing the gain in lift increases as the separation point is moved on the lower surface farther and farther from the leading edge.

On the other hand, this increased gain in lift requires higher angle of attack as the intersection of the curves and the minimum α/ε values indicate. This is consistent with the fact (already discussed in section 4.2) that the vortex system delays its appearance as the separation point is moved on the lower surface. To better understand why the curves intersect each other let us consider two specific ones, namely the one for $\delta_y = 0.05(l)$ and the one for $\delta_y = 0.02(l)$ for the ellipse.

Below $(\alpha/\varepsilon) = 1.99$, there can be no vortex system for $\delta_y = 0.05$ while there is one for $\delta_y = 0.02$. Therefore, despite the fact that the vortex strength will grow faster for $\delta = 0.05$ from the moment of its appearance, the vortex system for $\delta = 0.02$ has already been formed at lower angles of attack. As a result of this pre-existence there is a certain range of α/ε ($1.4 \leq \alpha/\varepsilon \leq 2.33$) in which the vortex system for the lower δ_y provides more lift until, at $\alpha/\varepsilon = 2.33$ the vortex system for the higher δ_y catches up.

Figure (10) shows the change in lift for various positions of the separation point. The lift for $\delta_y = 0$ (i.e. separation from the leading edge), has been taken as reference.

5. CONCLUSIONS

An extension of the "single line vortex with a straight feeding vortex sheet" model to delta wings with elliptical cross-section, as well as a study of the effect of the position of the separation points on the formation of the vortex system, leads to the following conclusions regarding the lift generated on such wings :

(i) The lift curve slope of a delta wing with elliptical cross-section goes up with increasing thickness. However this advantage cannot be realized at small angles of attack due to the increased difficulty in the formation of the vortex system.

(ii) Significant gain in lift can be realized by forcing the separation point away from its natural position on the upper surface of the wing (as it is known to be from experiments) towards the leading edge or even farther on the wing's lower surface. Again, this advantage has the same angle of attack limitations as mentioned above.

REFERENCES

1. Nielsen, J.N."Missile Aerodynamics", Mc Graw-Hill book company inc., 1960.
2. Brown, C.E. and Michael, W.H. "On Slender Delta Wings with Leading-Edge Separation", NACA TN-3430, April 1955.
3. Smith, J.H.B. "Improved calculations of Leading Edge Separation from Slender Delta Wings", Proc. Roy. Soc. A., Vol.306, pp67–90, 1968.
4. Bryson, A.E. "Symmetric Vortex Separation on Circular Cylinders and Cones", Journal of Applied Mechanics, pp643–648, December 1959.
5. Jorgensen, L.H. "Elliptic Cones Alone and with Wings at Supersonic Speeds", NACA TN-4045, October 1957.
6. Schindel, L.H "Separated Flow about Lifting Bodies", MIT TR-80, September 1963.
7. Friberg, E.G. "Measurement of Vortex Separation, part I : Two-Dimensional Circular and Elliptic Bodies", MIT TR-114, August 1965.
8. Friberg, E.G. "Measurement of Vortex Separation, part II : Three-Dimensional Circular and Elliptic Bodies", MIT TR-115, August 1965.
9. Schindel, L.H. "Effect of Vortex Separation on Lifting Bodies of Elliptic Cross-Section", MIT TR-118, September 1965.
10. Schindel, L.H. and Chamberlain, T.E. "Vortex Separation on Slender Bodies of Elliptic Cross-Section", MIT TR-138, August 1967.

FIGURES

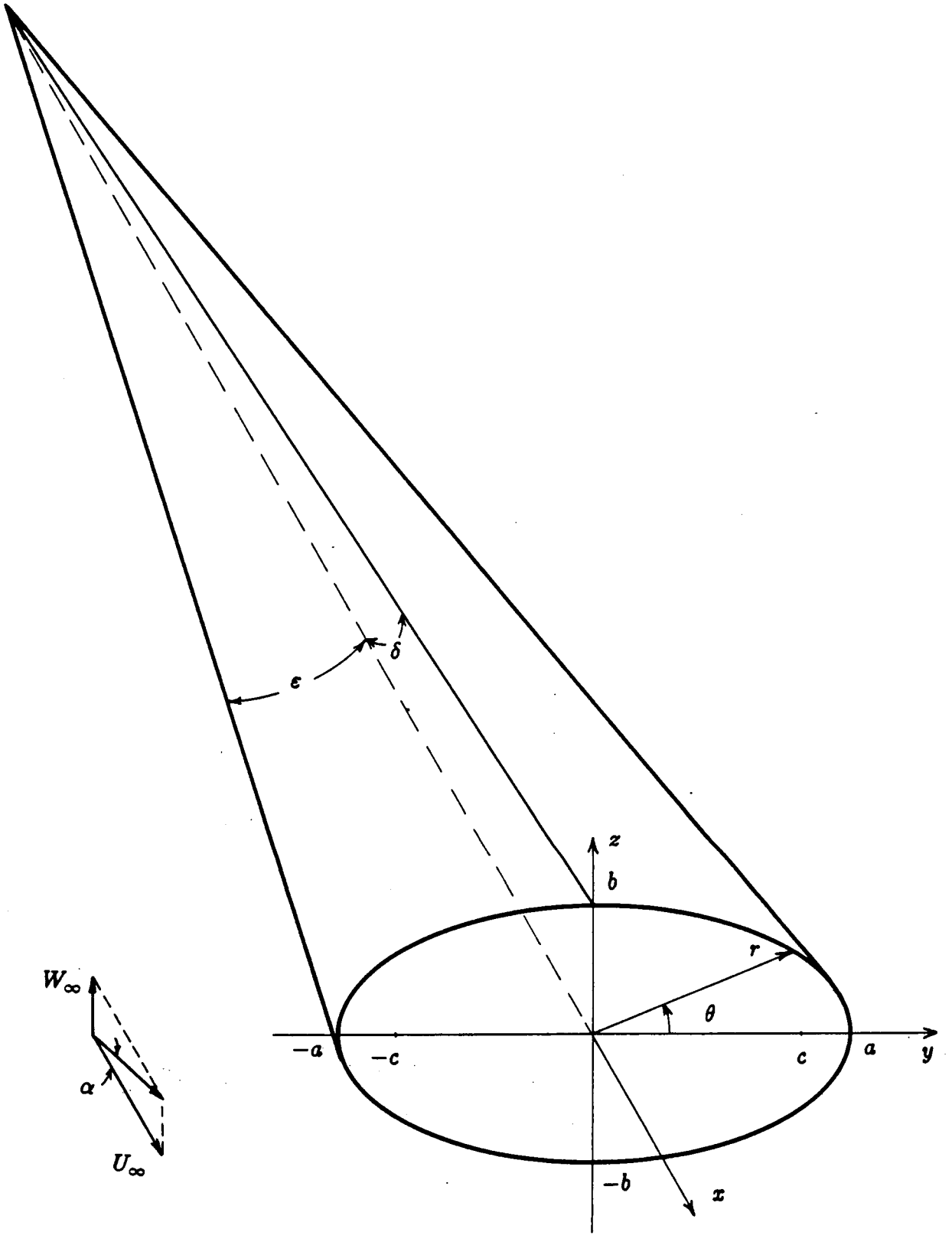

Figure 1. The geometry of a delta wing with elliptical cross-section.

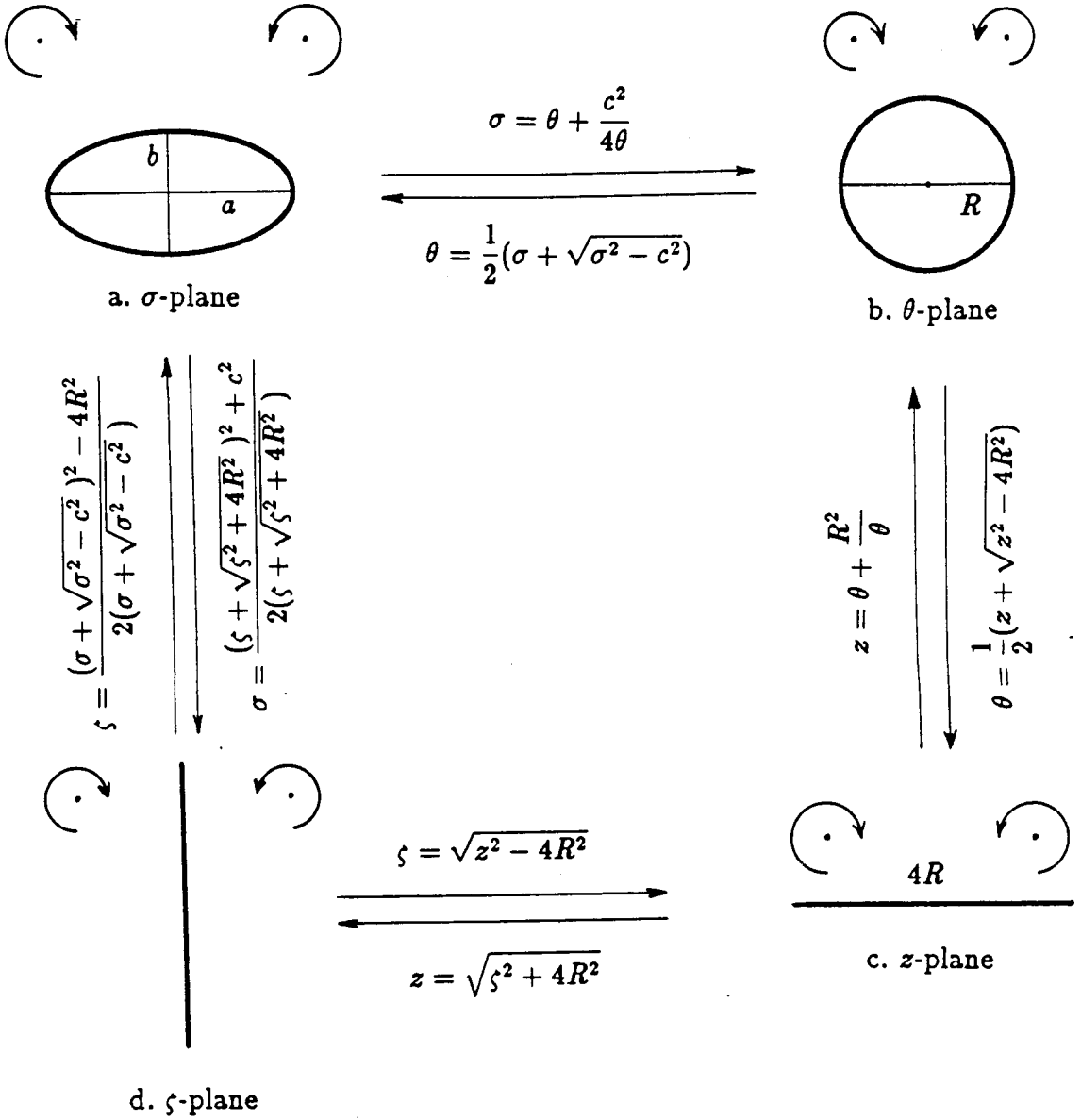

Figure 2. Conformal transformations used in the analysis of the cross-flow.

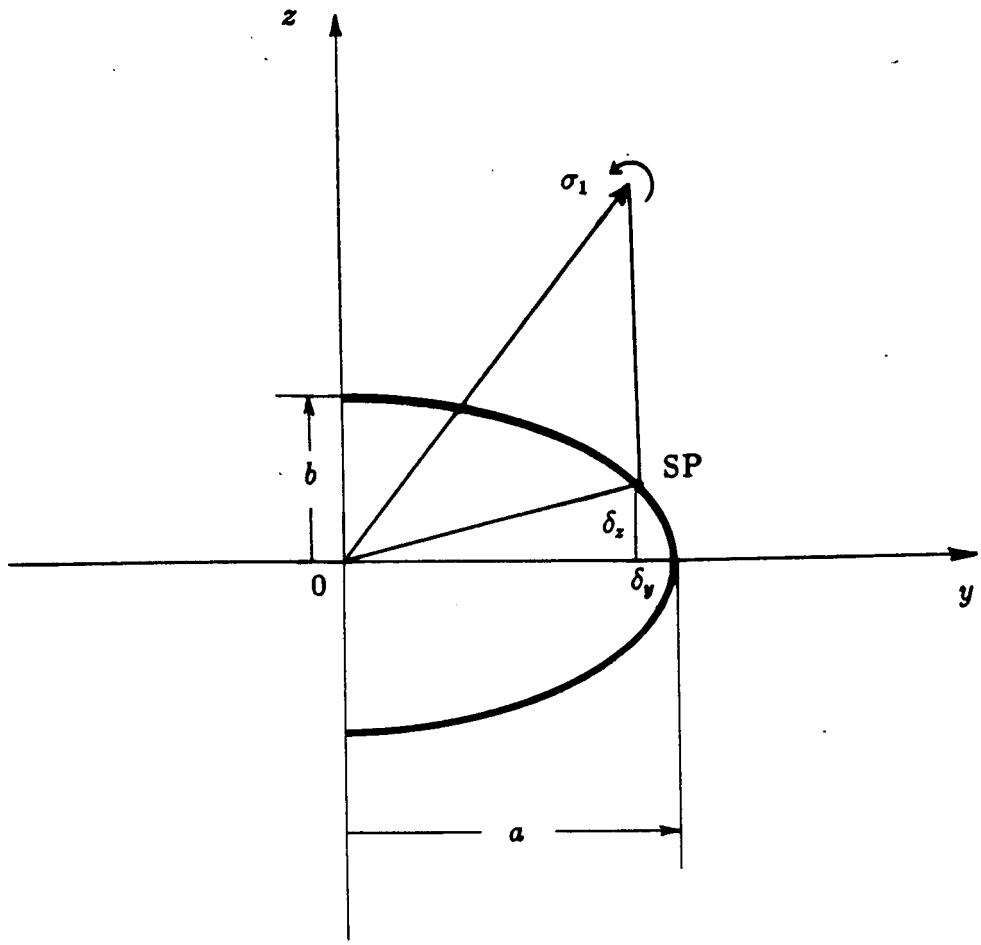

Figure 3. Schematic of the details in the cross-flow plane.

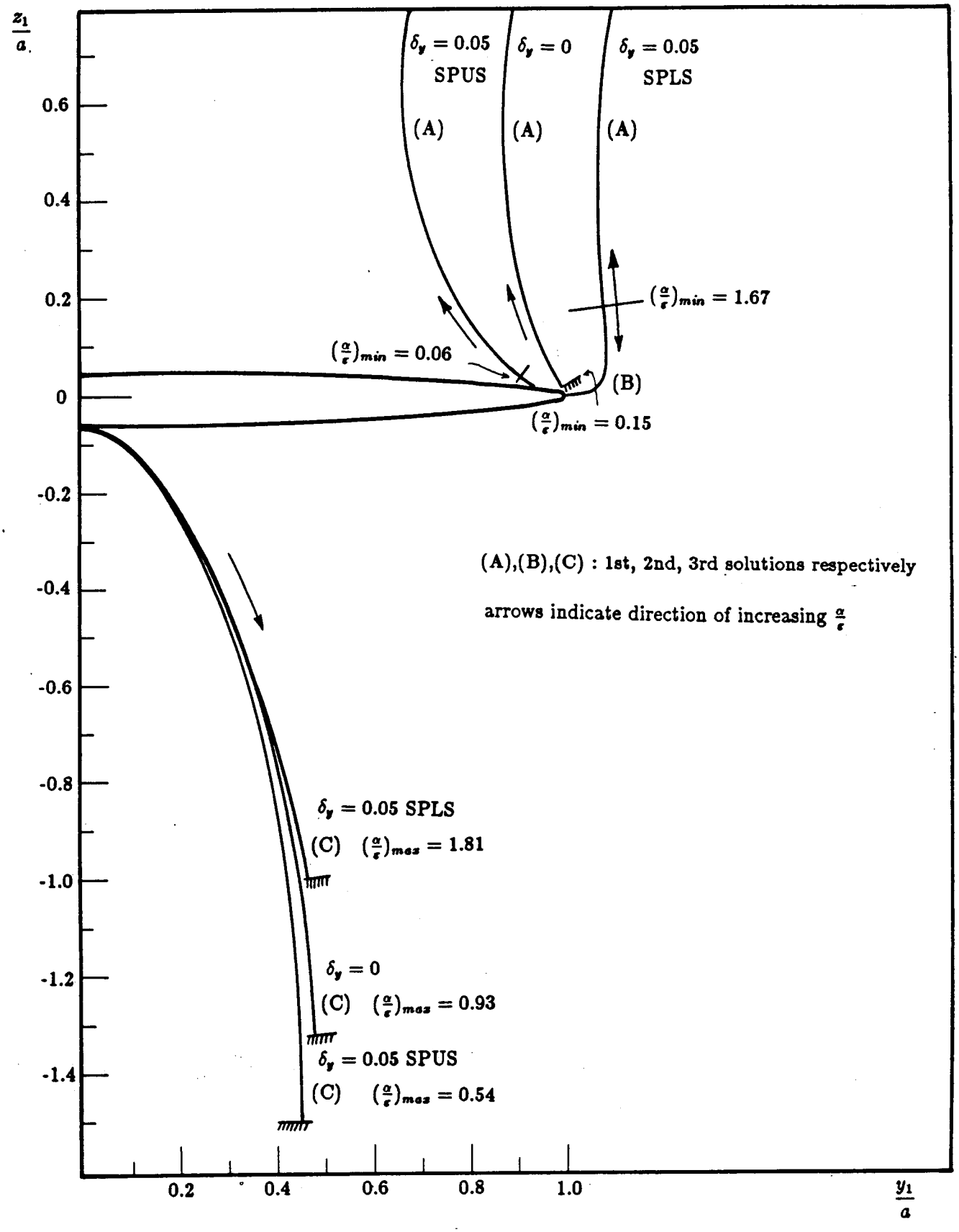

Figure 4. Vortex positions for a 5 per cent thick elliptical cross-section.

Figure 5. $(\alpha/\varepsilon)_{min}$ vs.distance of the SP from the LE of the wing.

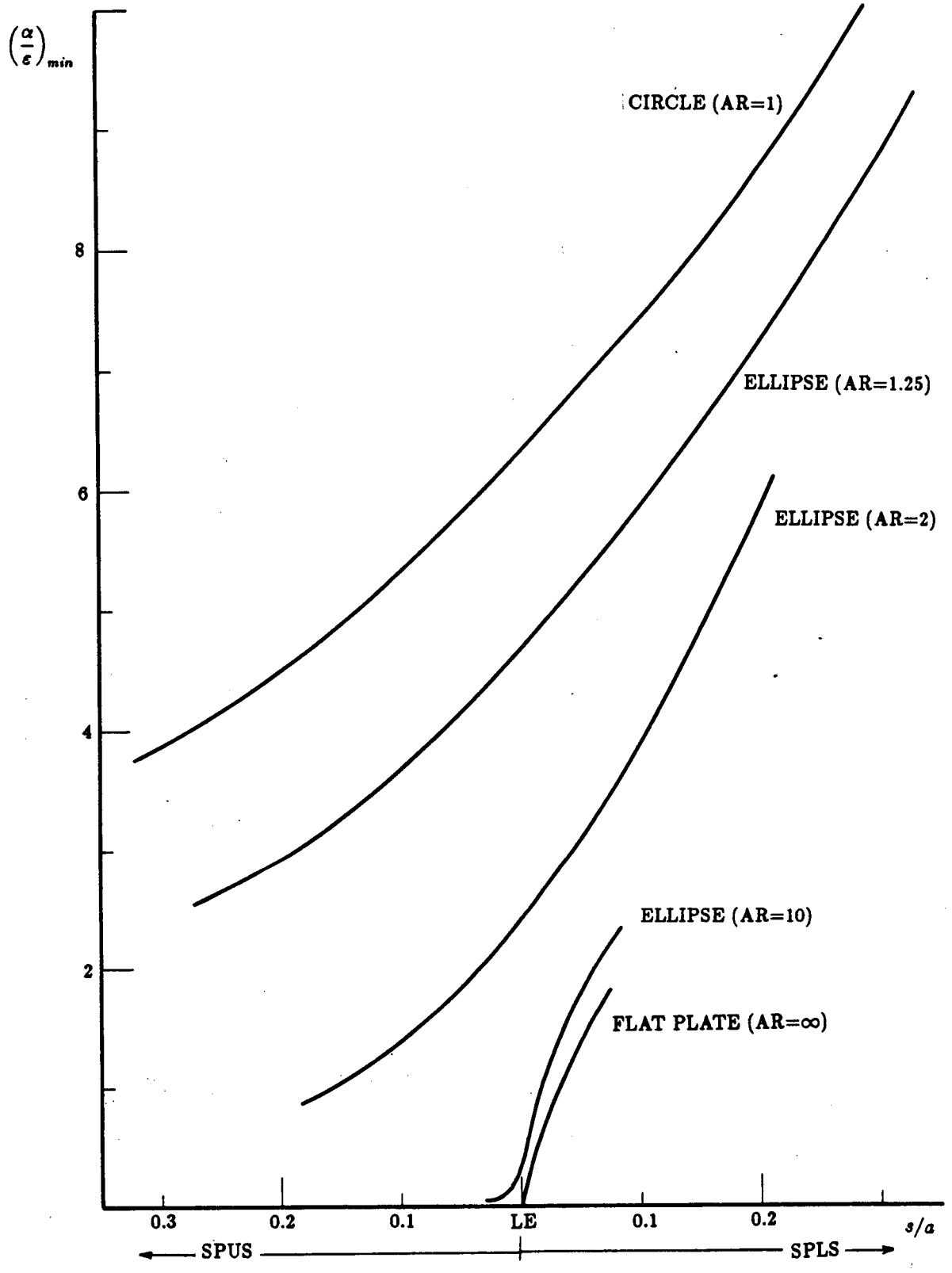

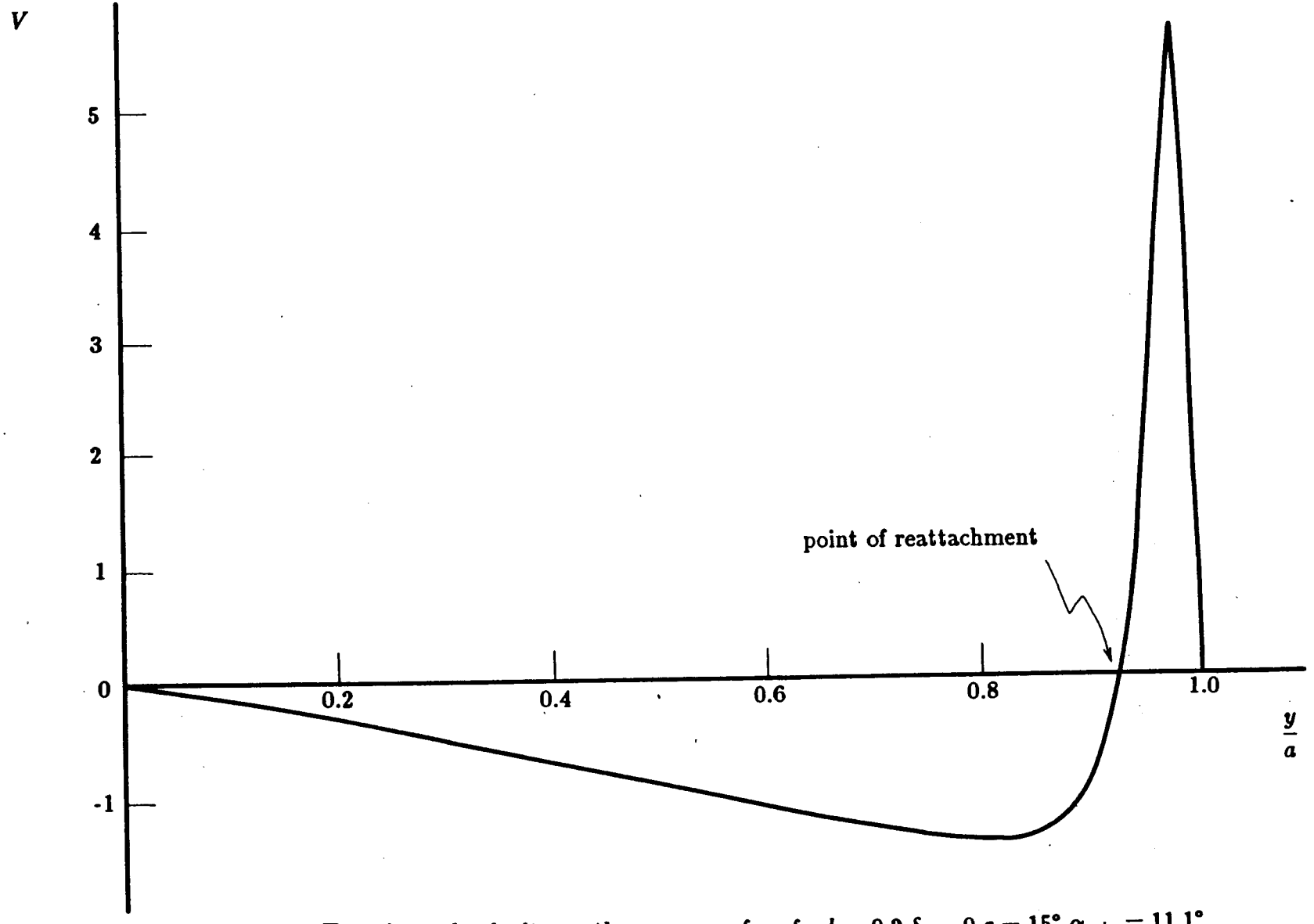

Figure 6a. Transformed velocity on the upper surface for $b = 0.2, \delta_y = 0, \varepsilon = 15°, \alpha_{min} = 11.1°$

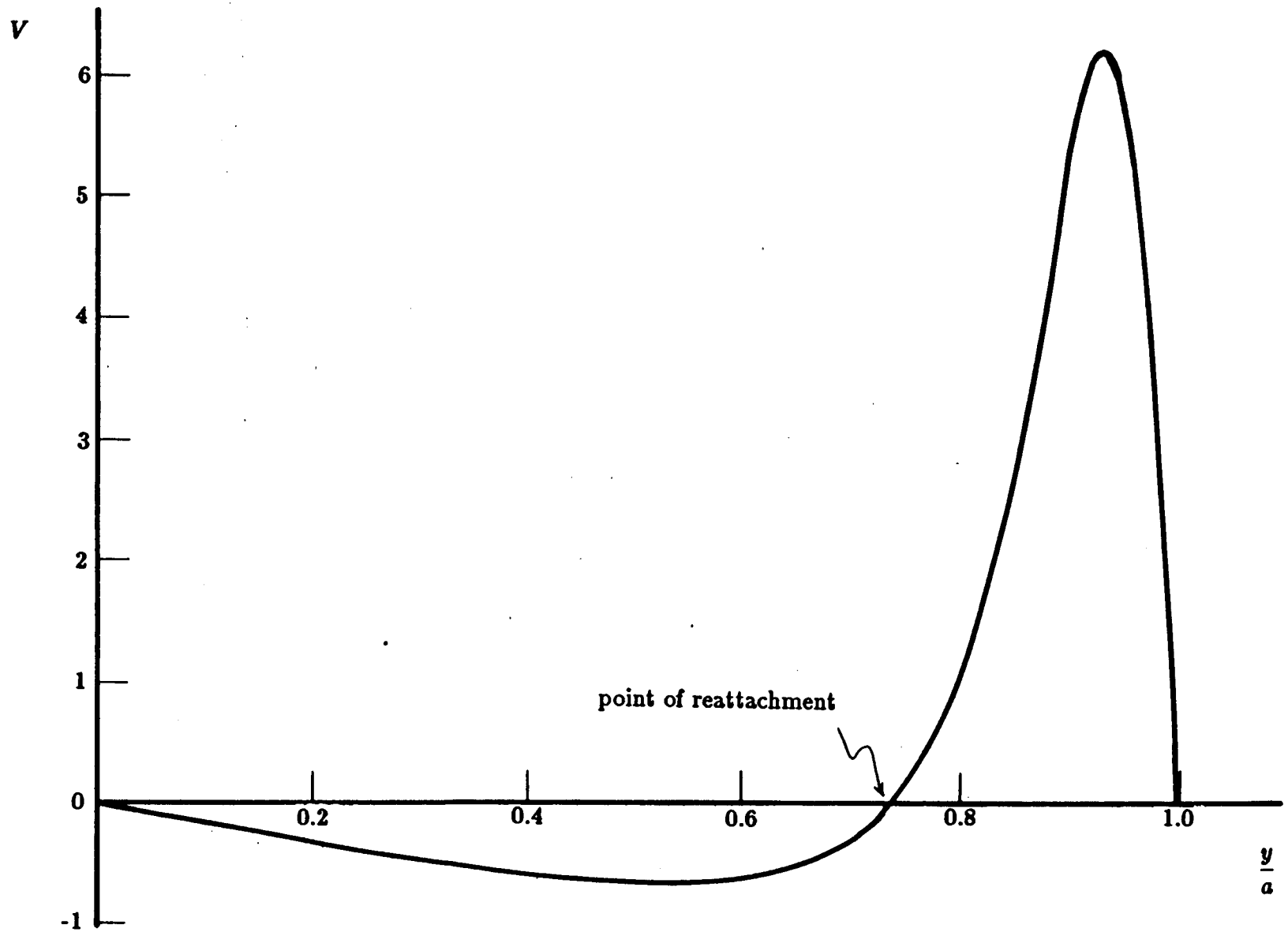

Figure 6b. Transformed velocity on the upper surface for $b = 0.2, \delta_y = 0, \varepsilon = 15°, \alpha = 15°$

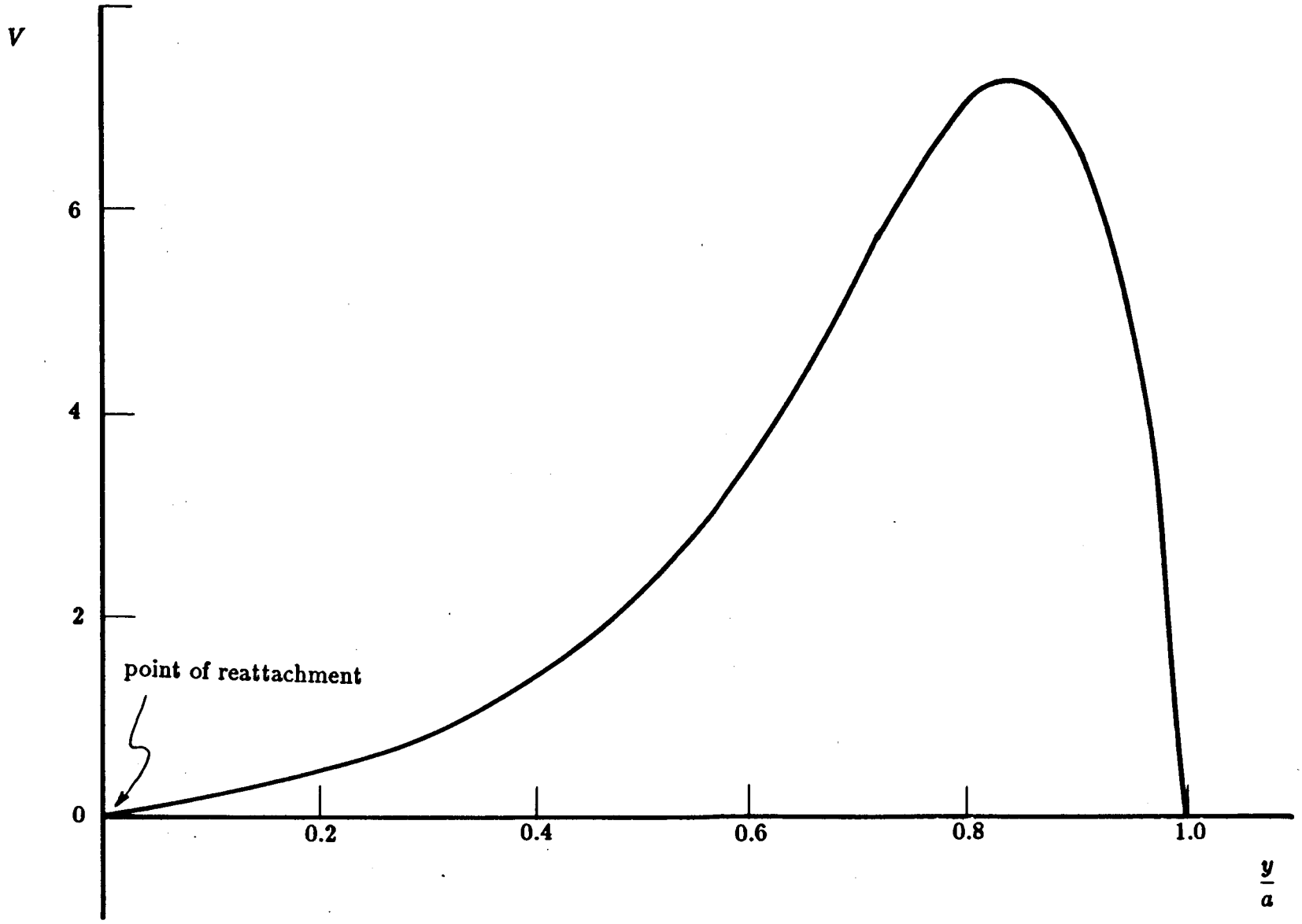

Figure 6c. Transformed velocity on the upper surface for $b = 0.2, \delta_y = 0, \epsilon = 15°, \alpha = 30°$

Figure 7a. Pressure distribution for $b = 0$, $\varepsilon = 15°$, $\alpha = 7.5°$, $\delta_y = 0$

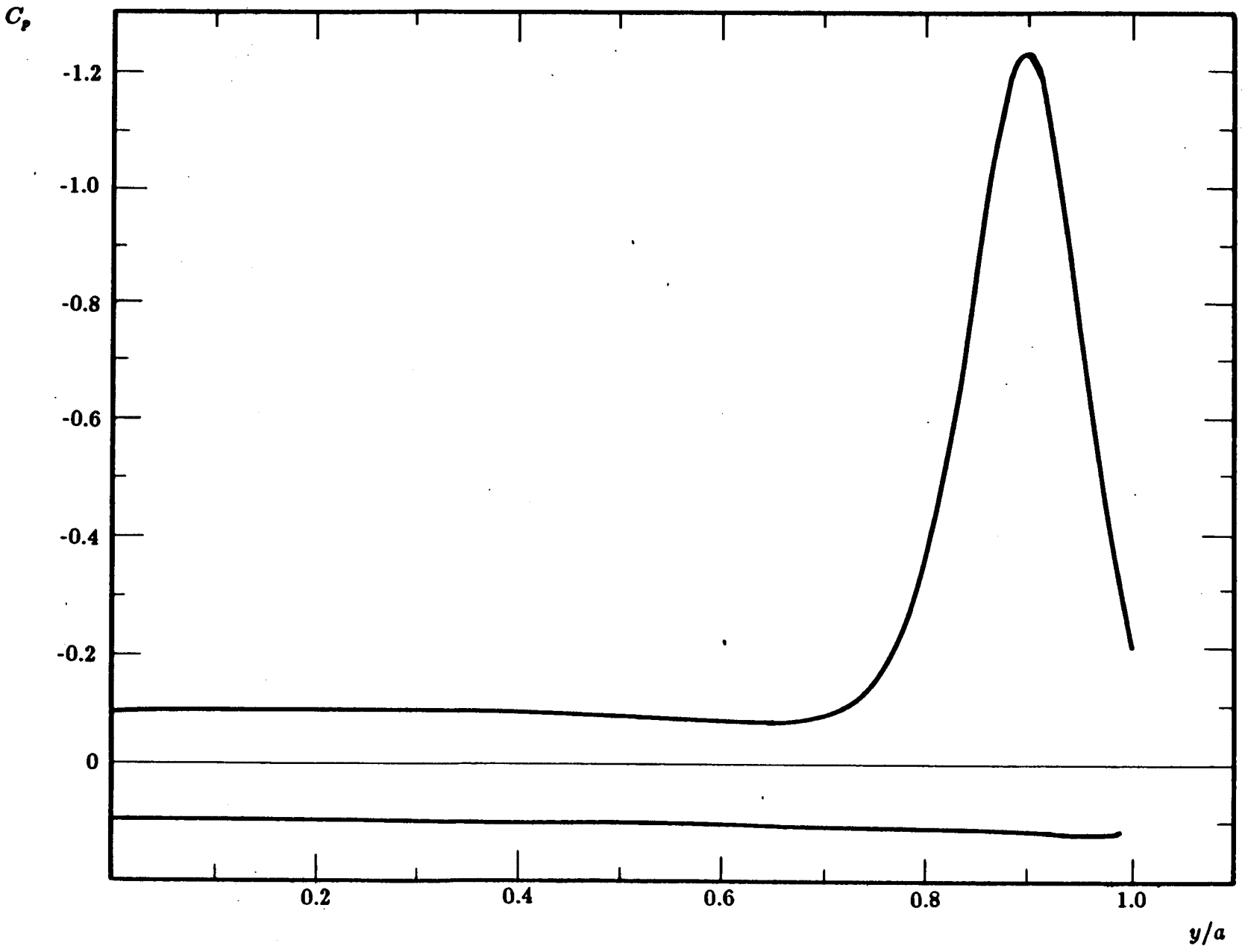

Figure 7b. Pressure distribution for $b = 0$, $\varepsilon = 15°$, $\alpha = 15°$, $\delta_y = 0$

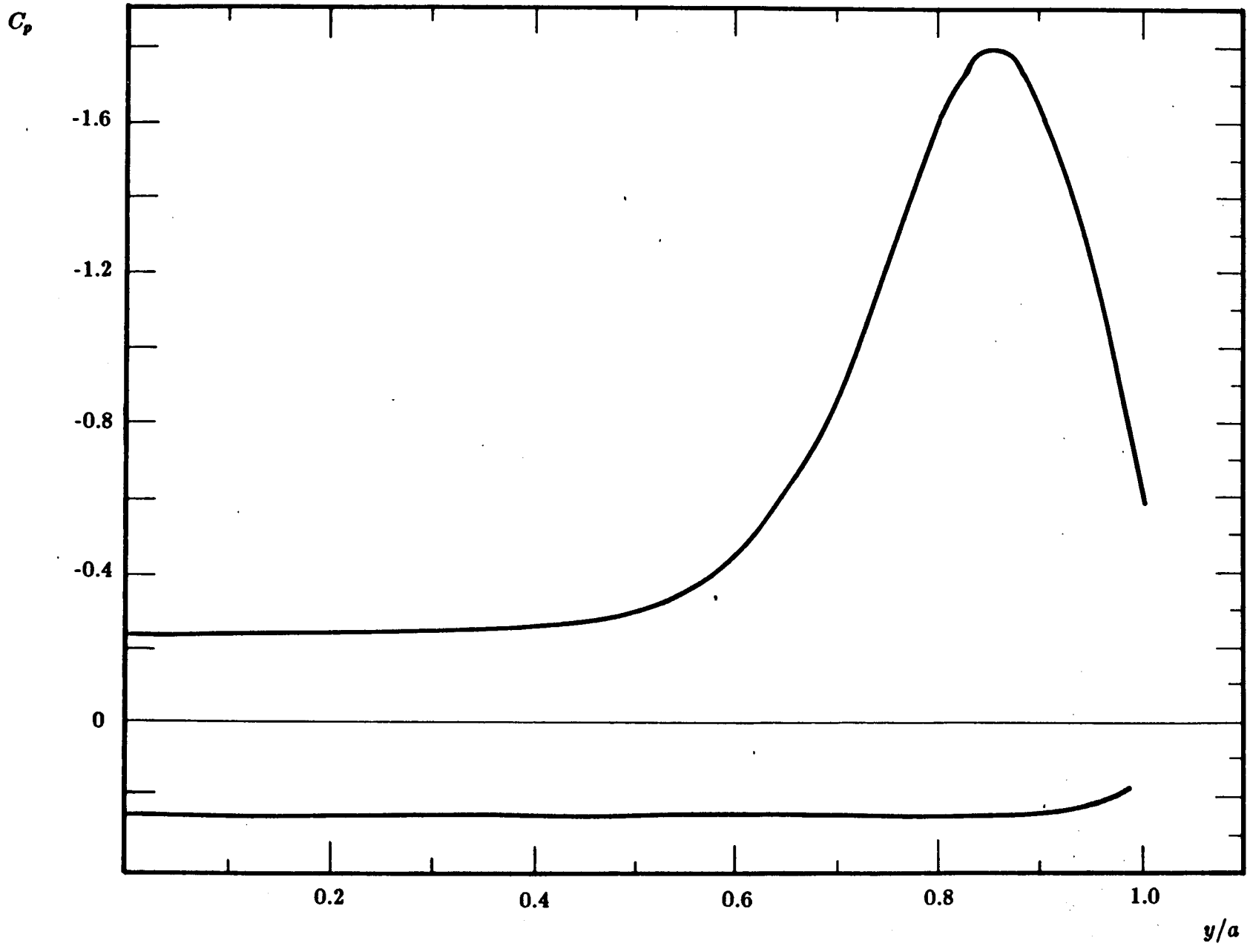

Figure 7c. Pressure distribution for $b = 0$, $\epsilon = 15°$, $\alpha = 30°$, $\delta_y = 0$

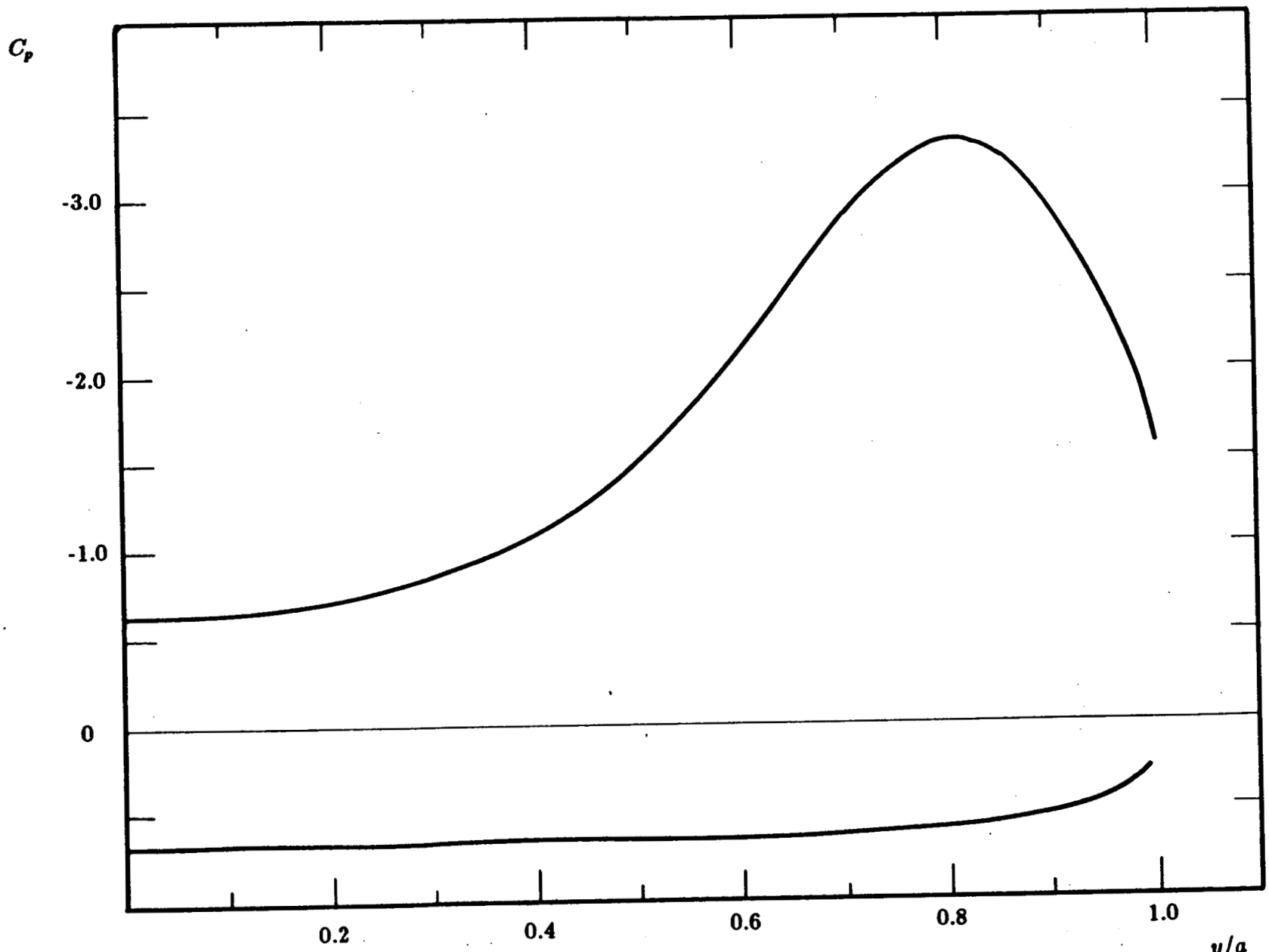

Figure 7d. Pressure distribution for $b = 0.1$, $\varepsilon = 15°$, $\alpha = 7.5°$, $\delta_y = 0$

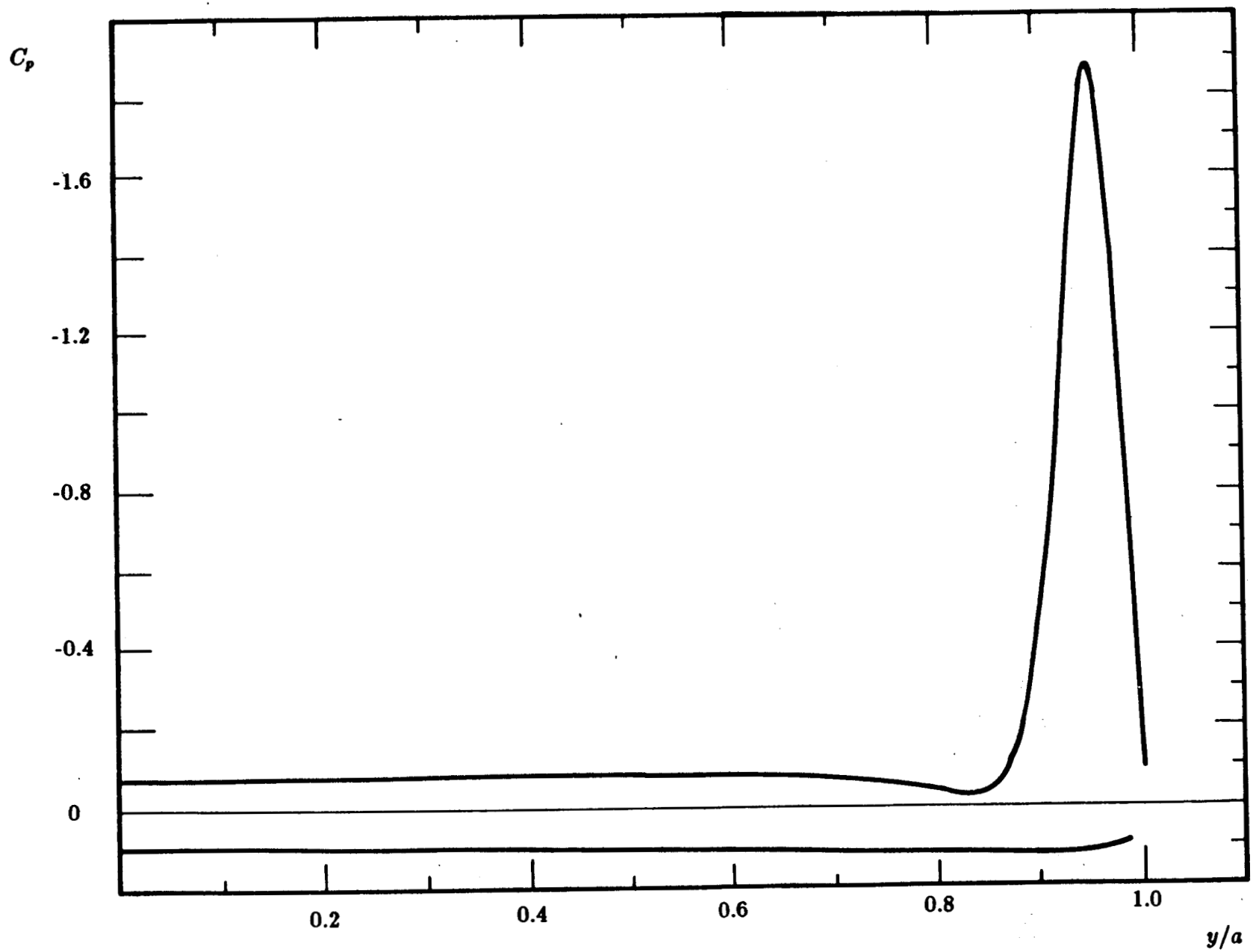

Figure 7e. Pressure distribution for $b = 0.1$, $\varepsilon = 15°$, $\alpha = 15°$, $\delta_y = 0$

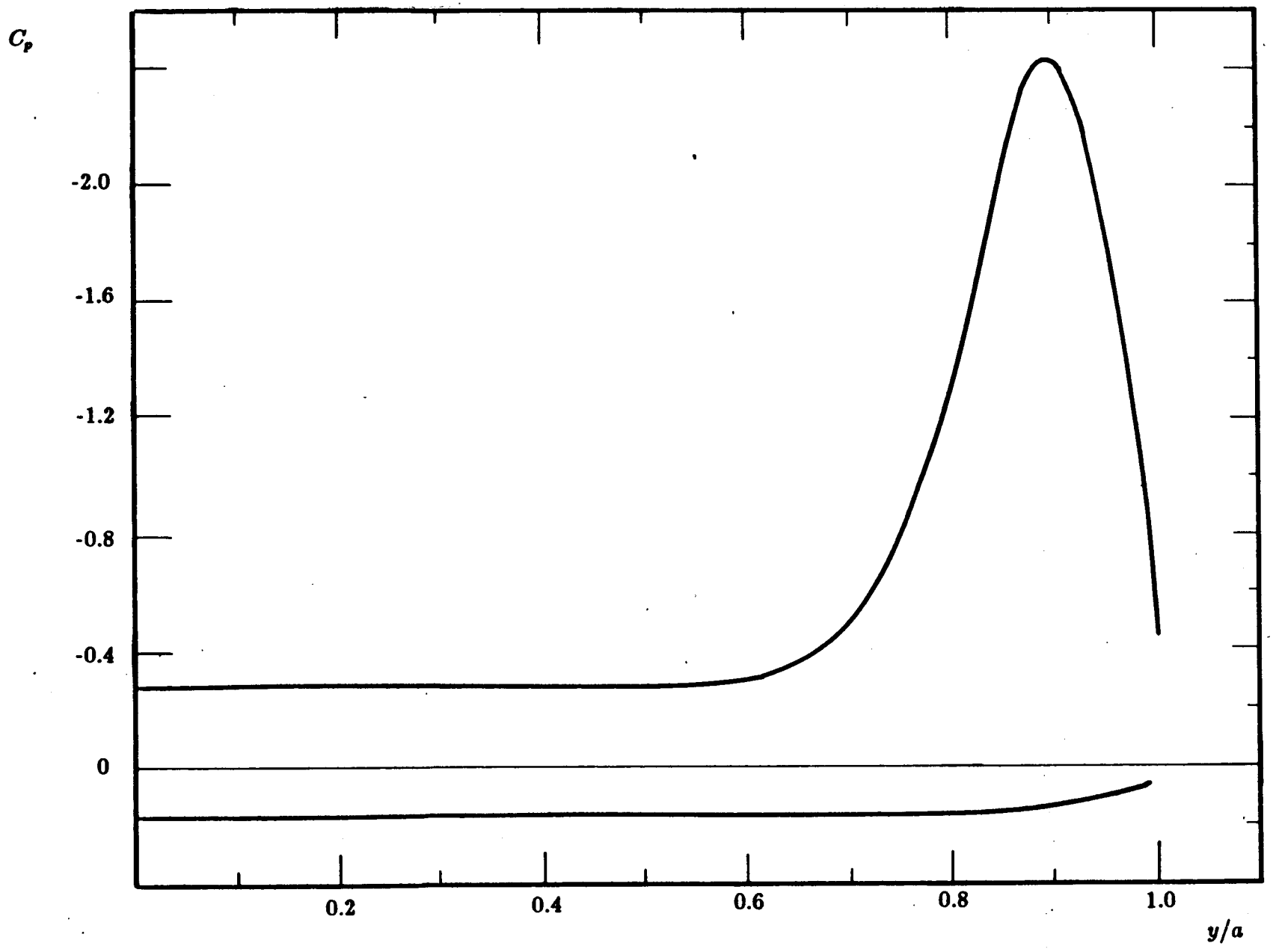

Figure 7f. Pressure distribution for $b = 0.1$, $\varepsilon = 15°$, $\alpha = 30°$, $\delta_y = 0$

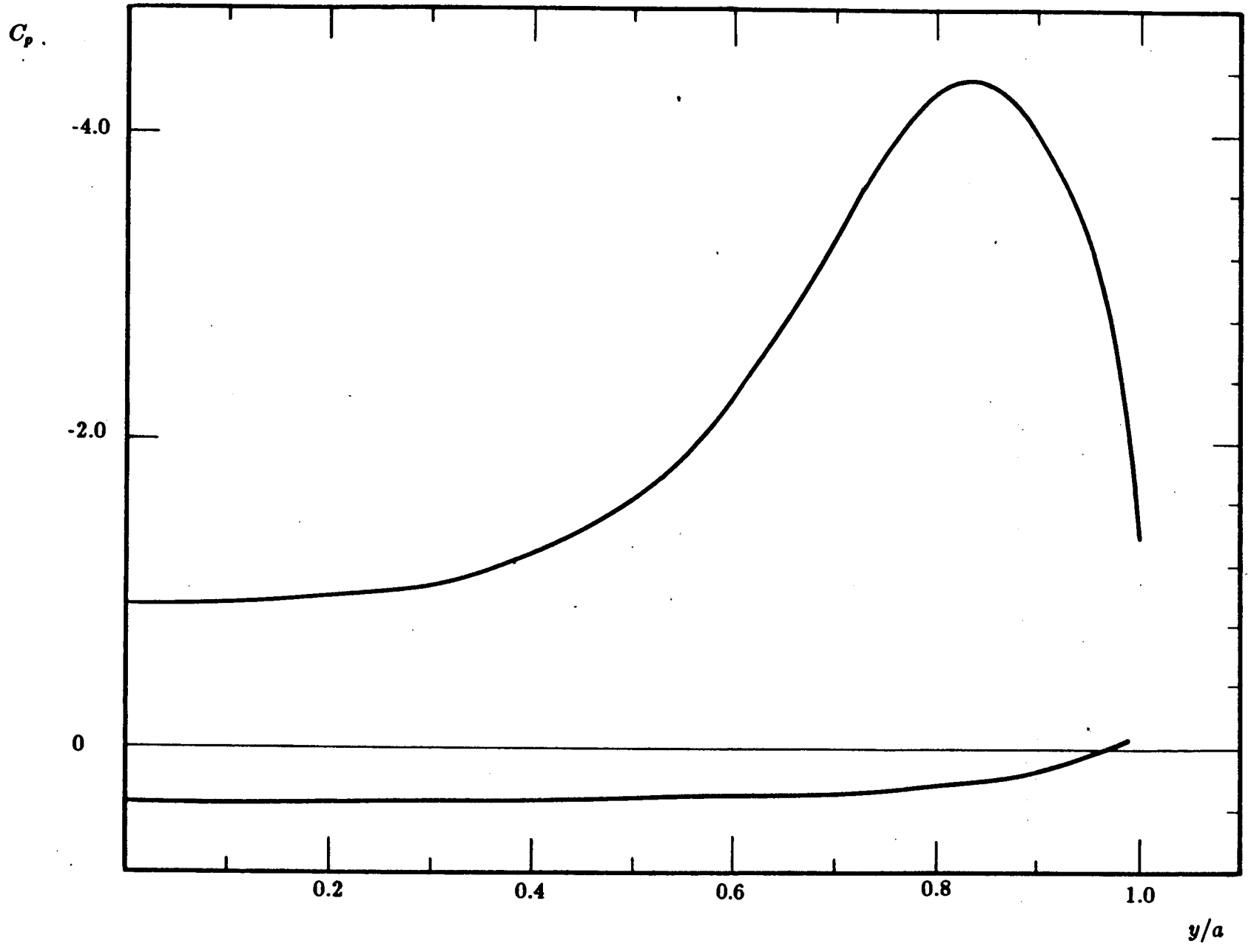

Figure 7g. Pressure distribution for $b = 0.2$, $\epsilon = 15°$, $\alpha = 15°$, $\delta_y = 0$

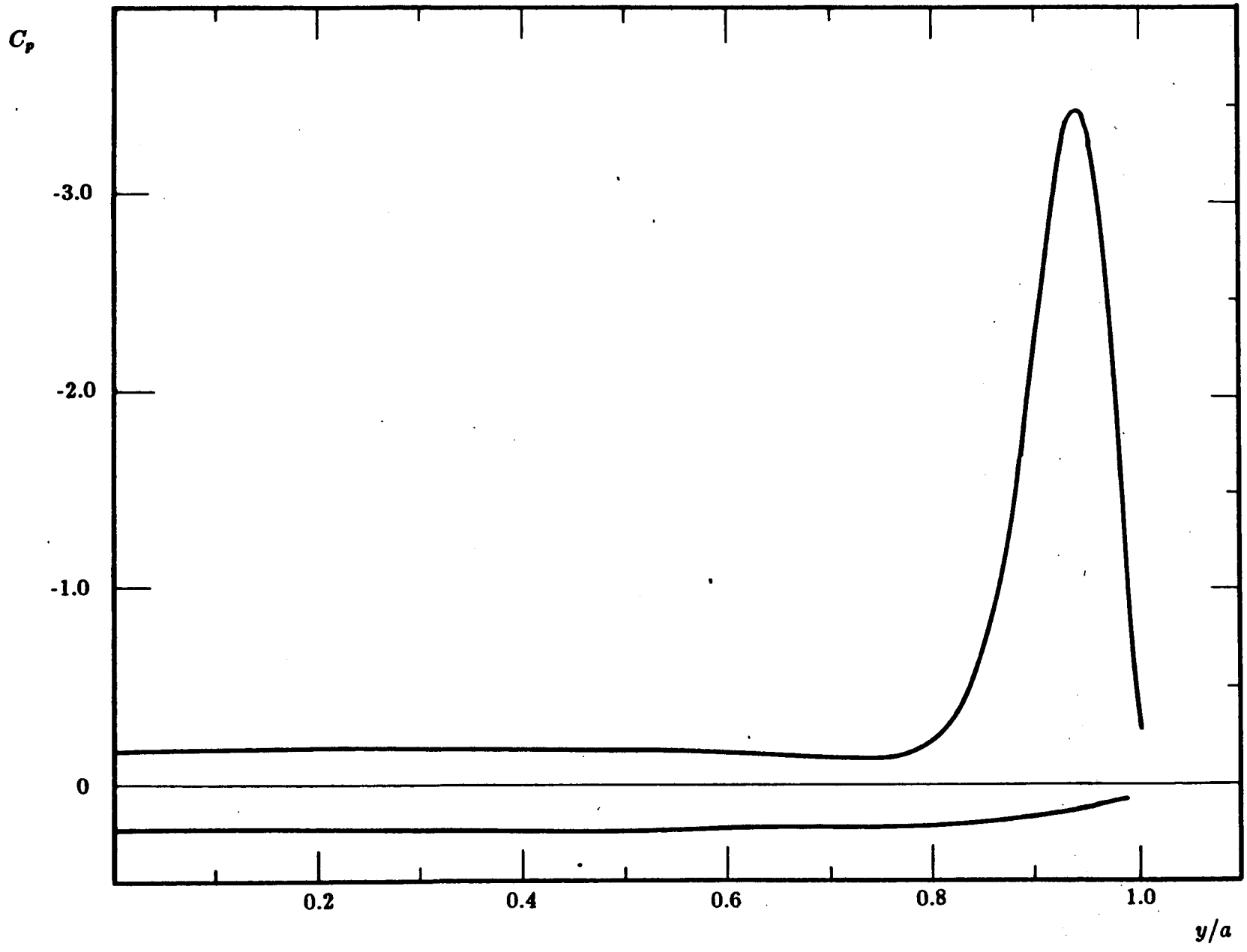

Figure 7h. Pressure distribution for $b = 0.2$, $\varepsilon = 15°$, $\alpha = 30°$, $\delta_y = 0$

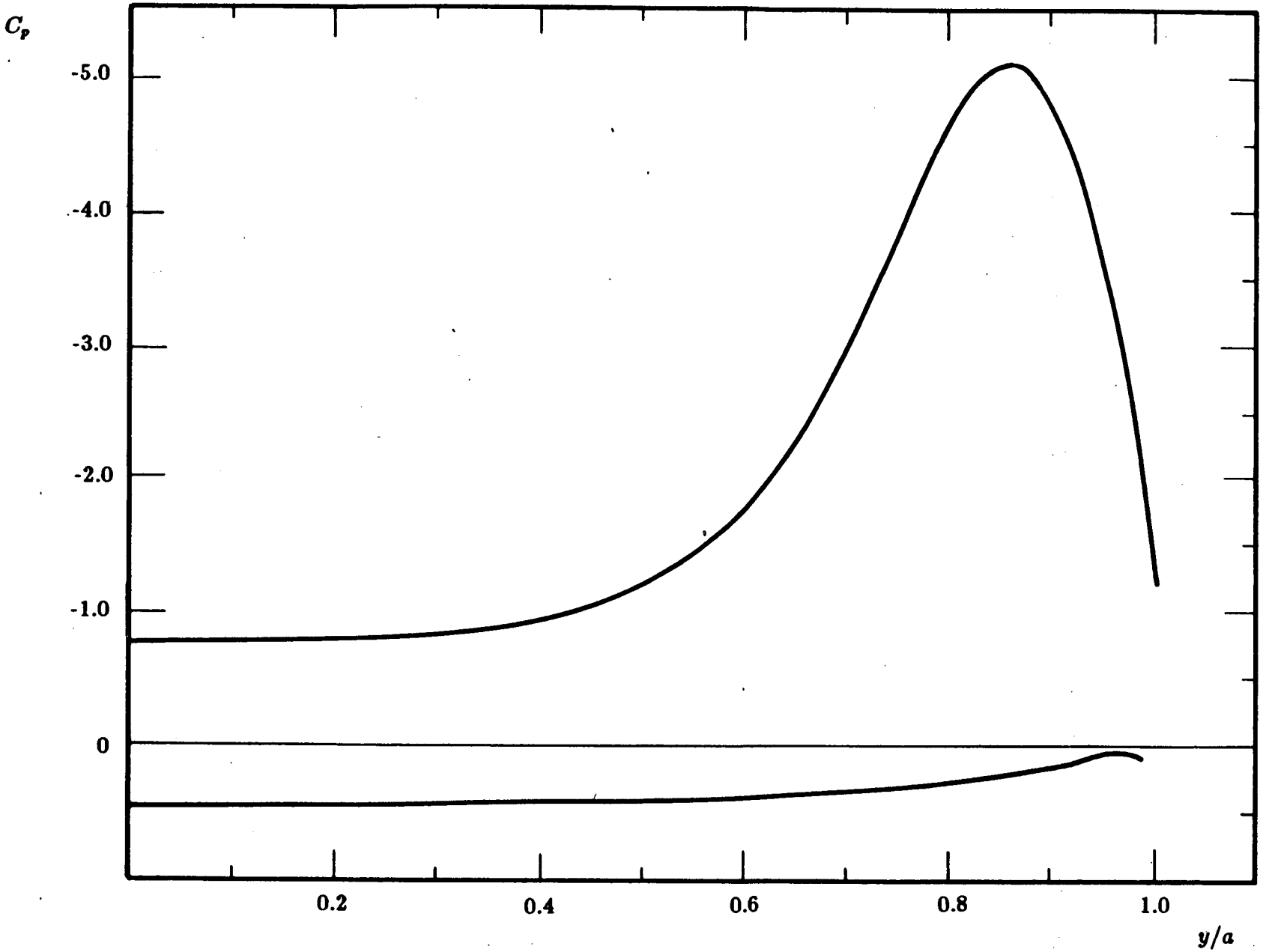

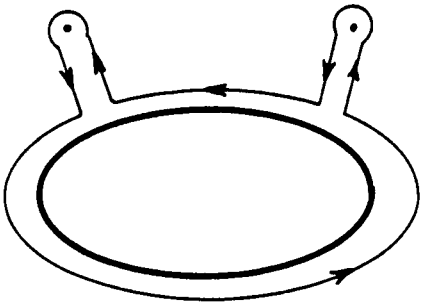

a. σ-plane

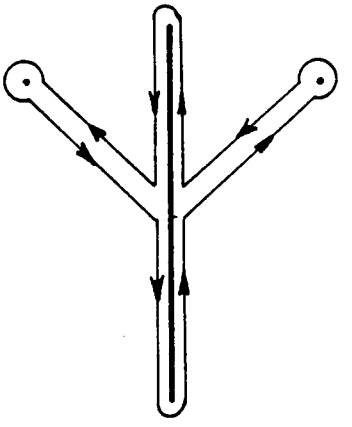

b. ς-plane

Figure 8. Contours of integration for the normal force.

Figure 9a. Lift coefficient vs. angle of attack for a flat cross-section.

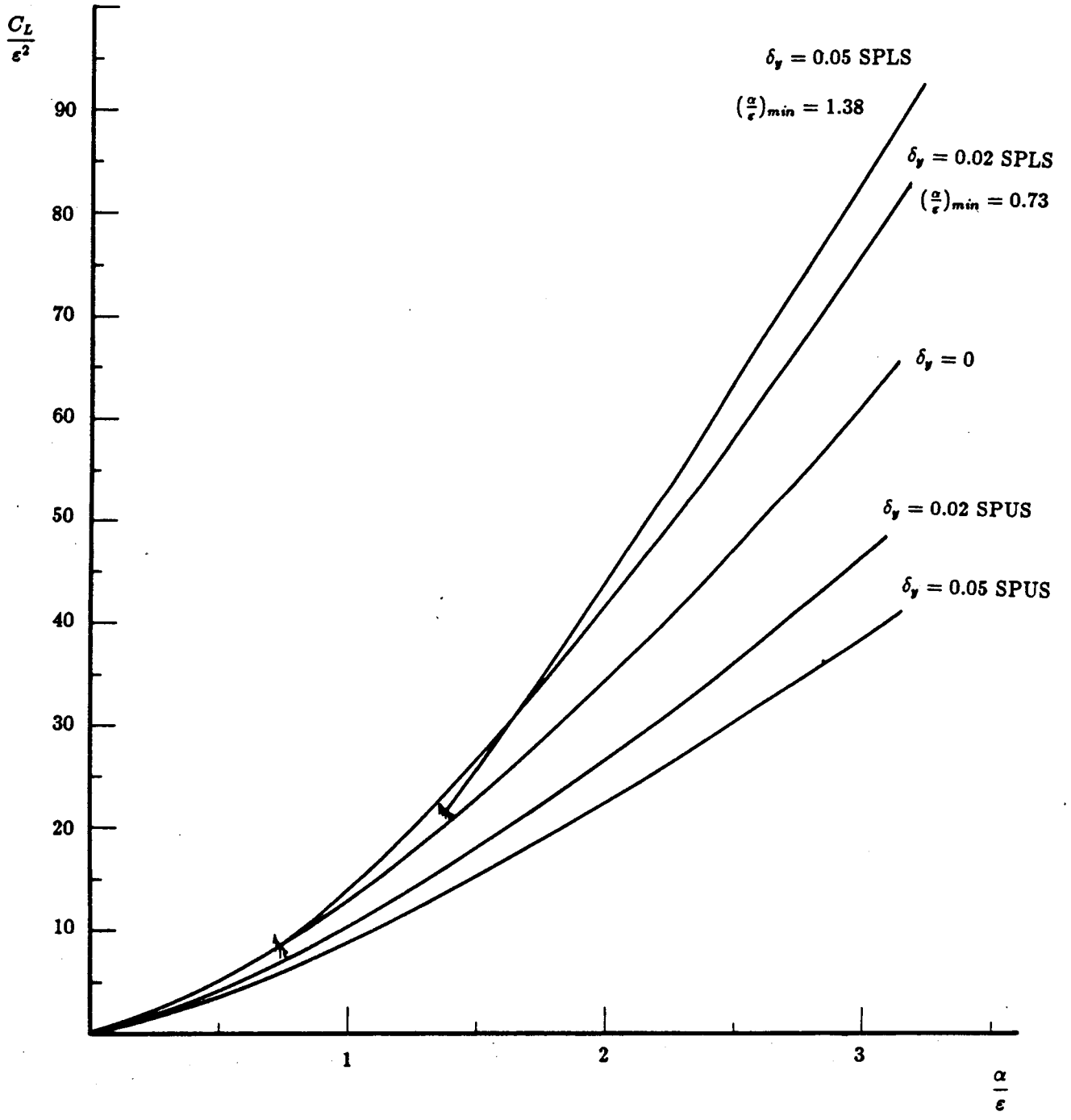

Figure 9b.

Lift coefficient vs. angle of attack for an elliptical cross-section 10 per cent thick.

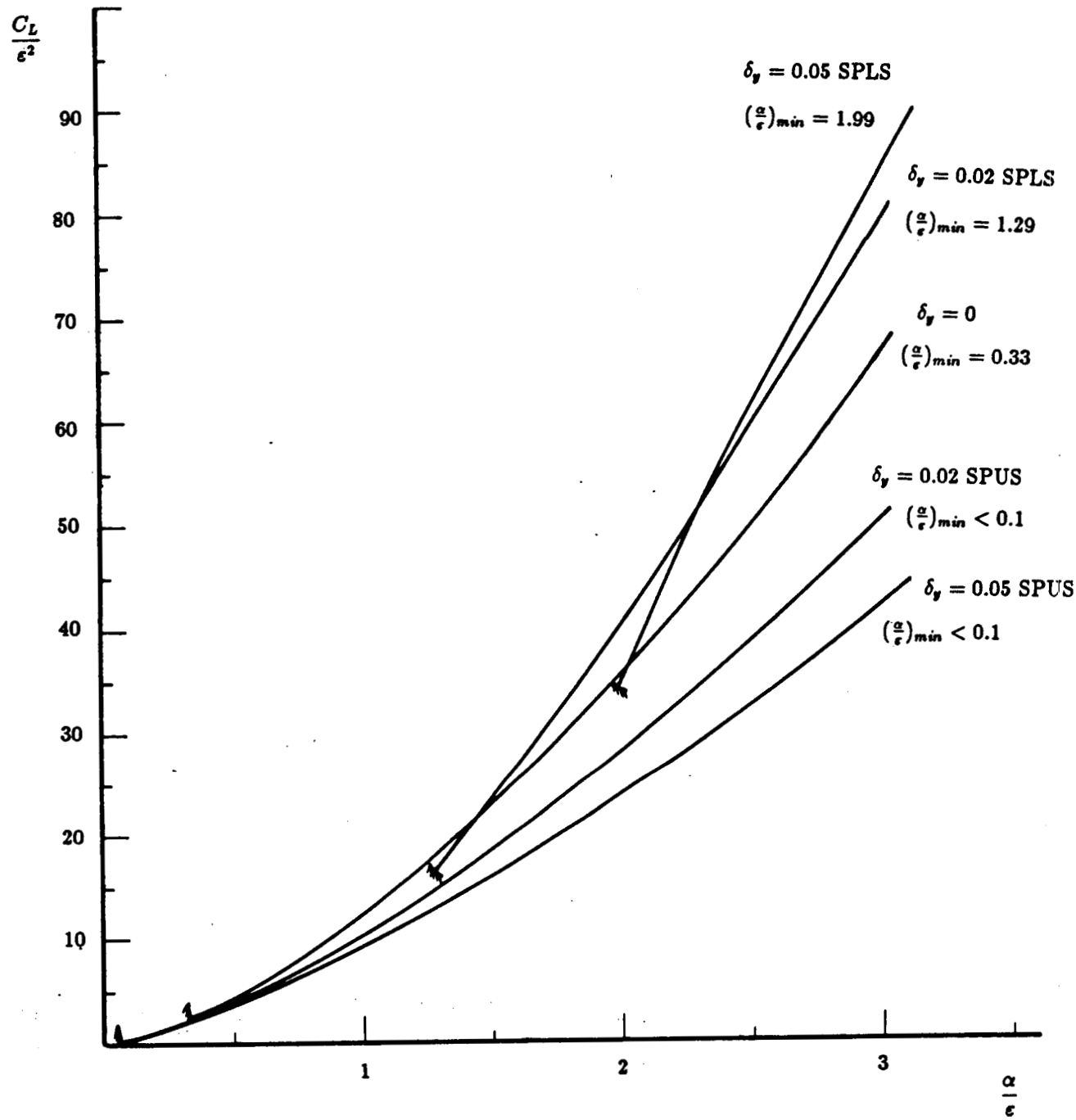

Figure 10a. Change of the lift coefficient vs. position of the SP for a flat plate.

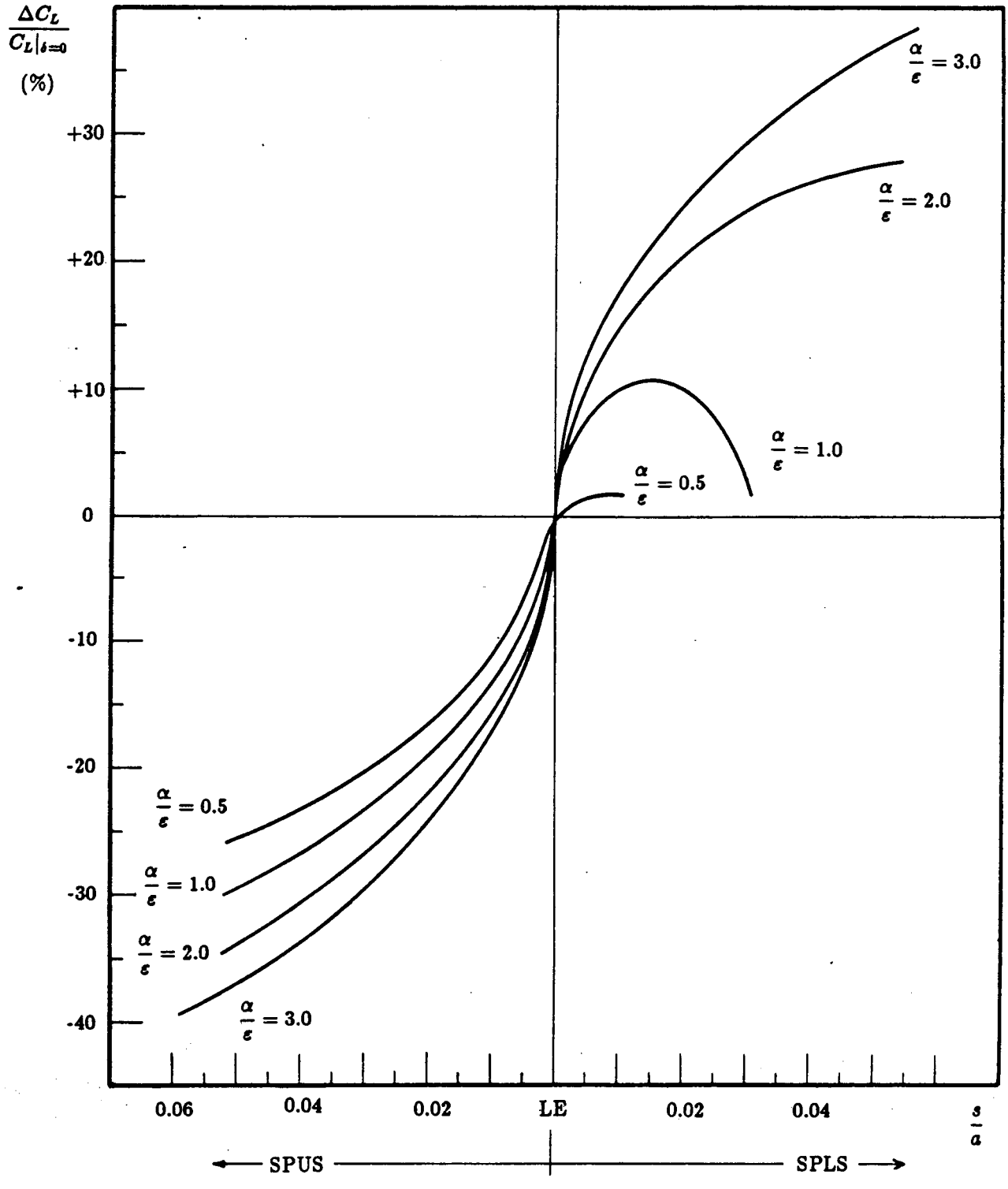

Figure 10b. Change of the lift coefficient vs. position of the SP for an elliptical cross-section 10 per cent thick.

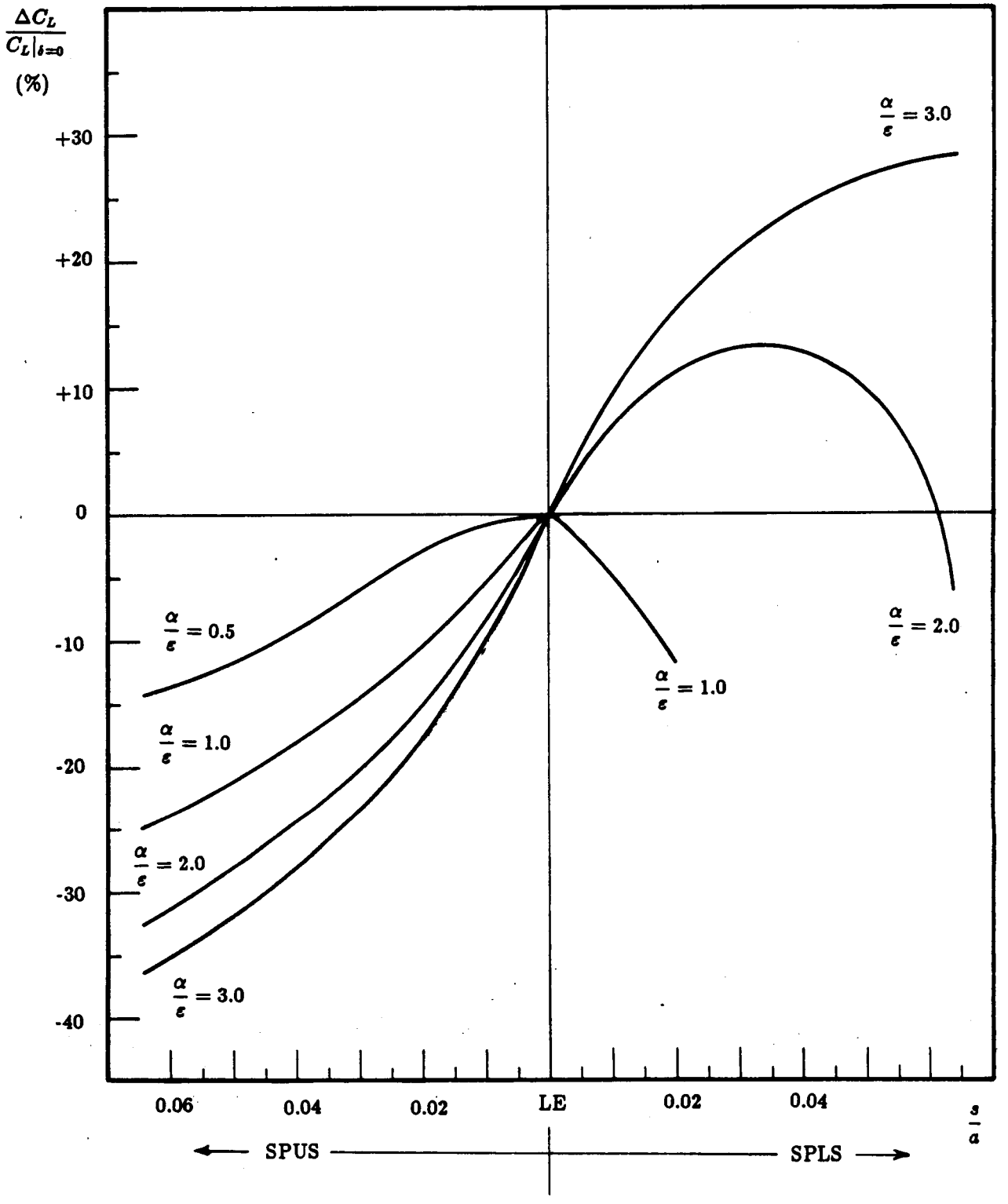

APPENDIX 1 : The Complex Potential for an Expanding Ellipse

In reference 1, the complex potential for an expanding ellipse is given by :

$$w_s(\sigma) = U_\infty b_0(x) + U_\infty \frac{S'(x)}{2\pi} \ln \frac{\sigma + \sqrt{\sigma^2 - c^2}}{2} \qquad (A1.1)$$

and since for an elliptical cone :

$$S(x) = \pi ab \qquad (A1.2)$$

$$a = x \tan \varepsilon \simeq x\varepsilon \qquad (A1.3)$$

$$b = x \tan \delta \simeq x\delta \qquad (A1.4)$$

we get :

$$S'(x) \simeq 2\pi x\varepsilon\delta = 2\pi a\delta = 2\pi b\varepsilon \qquad (A1.5)$$

Also, $b_0(x)$ is defined as :

$$b_0(x) = a_0(x) \ln \frac{\beta}{2} - \frac{1}{2} \int_{0+}^{x} a_0'(\xi) \ln (x - \xi) d\xi + \frac{1}{2} \int_{x}^{1-} a_0'(\xi) \ln (\xi - x) d\xi$$

$$-\frac{1}{2}a_0(0^+)\ln x - \frac{1}{2}a_0(1^-)\ln(1-x) \qquad (A1.6)$$

where

$$a_0(x) = \frac{S'(x)}{2\pi} \simeq b\varepsilon \qquad (A1.7)$$

$$a_0'(x) = \frac{S''(x)}{2\pi} \simeq \varepsilon\delta$$

and for incompressible flow :

$$\beta = 1$$

The first integral in equation (A1.6) becomes :

$$\frac{1}{2}\varepsilon\delta \int_{0+}^{x} \ln(x-\xi)d\xi = \frac{1}{2}\varepsilon\delta x(\ln x - 1)$$

while the second integral in equation (A1.6) gives :

$$\frac{1}{2}\varepsilon\delta \int_{x}^{1^-} \ln(\xi - x)d\xi = \frac{1}{2}\varepsilon\delta(1-x)[\ln(1-x) - 1]$$

for the last two terms in equation (A1.6) we have :

$$a_0(0^+) = \lim_{x\to 0^+} a_0(x) = 0$$

$$a_0(1^-) = \lim_{x \to 1^-} a_0(x) = \varepsilon\delta$$

and equation (A1.6) gives :

$$b_0(x) = -\varepsilon\delta \left\{ x \left[\ln 2\sqrt{x(1-x)} - 1 \right] + \frac{1}{2} \right\} \qquad (A1.8)$$

Substituting equations (A1.5) and (A1.8) into equation (A1.1), we finally get for the complex potential of an ellipse that expands in a conical manner :

$$w_s(\sigma) = -U_\infty \varepsilon\delta \left\{ x \left[\ln 2\sqrt{x(1-x)} - 1 \right] + \frac{1}{2} \right\} + U_\infty b\varepsilon \ln \frac{\sigma + \sqrt{\sigma^2 - c^2}}{2} \qquad (A1.9)$$

APPENDIX 2 : Derivation of an Expression for the Separation Point Location

The distance of the separation point from the leading edge is given by :

$$\eta = \int d\eta = \int \sqrt{dy^2 + dz^2} \qquad (A2.1)$$

and since

$$\frac{y^2}{a^2} + \frac{z^2}{b^2} = 1 \Rightarrow \qquad (A2.2)$$

$$dz = -\frac{y}{z}\frac{b^2}{a^2}dy \qquad (A2.3)$$

$$\frac{y^2}{z^2} = \frac{y^2 a^2}{b^2(a^2 - y^2)} \qquad (A2.4)$$

equation (A2.1) gives :

$$\eta = \int_a^{a-\delta_y} \sqrt{1 + \frac{b^2}{a^2}\frac{y^2}{a^2 - y^2}}dy \qquad (A2.5)$$

and for $a = 1$:

$$\eta = \int_1^{1-\delta_y} \sqrt{1 + b^2\frac{y^2}{1 - y^2}}dy \qquad (A2.6)$$

or, since $c^2 = a^2 - b^2 = 1 - b^2$,

$$\eta = \int_1^{1-\delta_y} \sqrt{\frac{1-c^2y^2}{1-y^2}}\,dy \qquad (A2.7)$$

To avoid the evaluation of the elliptic integral of the second kind, the integrand will be simplified in the following manner :

$$\frac{1-c^2y^2}{1-y^2} = \frac{(1+cy)(1-cy)}{(1+y)(1-y)} \simeq \frac{(1+c)(1-cy)}{2(1-y)} \qquad (A2.8)$$

since close to the leading edge $y \simeq 1$.

Note that the above expression is valid for all thicknesses i.e. from the flat-plate case ($c = 1$) to the circle case ($c = 0$). Substituting equation (A2.8) into (A2.7) we get :

$$\eta = \sqrt{\frac{1+c}{2}} \int_1^{1-\delta_y} \sqrt{\frac{1-cy}{1-y}}\,dy \qquad (A2.9)$$

and integration by parts gives the final expression :

$$\eta = -\sqrt{\frac{1+c}{2}} \left\{ \sqrt{(1-c+c\delta_y)\delta_y} + \frac{c-1}{2\sqrt{c}} \ln \frac{[c-c\delta_y-1+\sqrt{(1-c+c\delta_y)c\delta_y}\,]^2}{(1-c)(1-c+c\delta_y)} \right\} \qquad (A2.10)$$

APPENDIX 3 : Evaluation of the derivative dw/da

For the term w_{s2} in equation (6) the derivative with respect to x can be evaluated directly :

$$\frac{dw_{s2}}{dx} = -U_\infty \varepsilon \frac{b}{x} \left\{ \ln \left[2\sqrt{x(1-x)} \right] - \frac{1}{2(1-x)} \right\} \qquad (A3.1)$$

For the rest of the complex potential $(w_{cf} + w_{s1})$ we have :

$$\frac{dw}{da} = \frac{\partial w}{\partial \theta}\frac{d\theta}{da} + \frac{\partial w_{cf}}{\partial \theta_1}\frac{d\theta_1}{da} + \frac{\partial w_{cf}}{\partial \bar{\theta}_1}\frac{d\bar{\theta}_1}{da} + \frac{\partial w_{cf}}{\partial k}\frac{dk}{da} + \frac{\partial w_{cf}}{\partial R}\frac{dR}{da} + \frac{\partial w_{s1}}{\partial b}\frac{db}{da} \qquad (A3.2)$$

and since $\theta_1, \bar{\theta}_1$ (or $\sigma_1, \bar{\sigma}_1$), k, a and b are all linear functions of x we have :

$$\frac{d\theta_1}{da} = \frac{\theta_1}{a} \qquad (A3.3)$$

$$\frac{d\bar{\theta}_1}{da} = \frac{\bar{\theta}_1}{a} \qquad (A3.4)$$

$$\frac{dR}{da} = \frac{R}{a} \qquad (A3.5)$$

$$\frac{db}{da} = \frac{b}{a} \qquad (A3.6)$$

while from equation (19) we get :

$$k = \frac{(t+\bar{\theta}_1)(t-\theta_1)(t\bar{\theta}_1 - R^2)(t\theta_1 + R^2)}{t^2(\theta_1+\bar{\theta}_1)(R^2-\theta_1\bar{\theta}_1)} U_\infty \alpha \qquad (A3.7)$$

so

$$\frac{dk}{da} = \frac{k}{a} \qquad (A3.8)$$

Now from equations (3) and (7) we get :

$$\frac{\partial w}{\partial \theta} = -\imath U_\infty \alpha \left(1 + \frac{R^2}{\theta^2}\right) - \imath k \left(\frac{1}{\theta-\theta_1} - \frac{1}{\theta+\bar{\theta}_1} + \frac{\theta_1}{\theta\theta_1 + R^2} - \frac{\bar{\theta}_1}{\theta\bar{\theta}_1 - R^2}\right) + U_\infty b \frac{\varepsilon}{\theta} \qquad (A3.9)$$

$$\frac{\partial w_{cf}}{\partial \theta_1} = \imath k \left(\frac{1}{\theta-\theta_1} - \frac{\theta}{\theta\theta_1 + R^2}\right) \qquad (A3.10)$$

$$\frac{\partial w_{cf}}{\partial \bar{\theta}_1} = \imath k \left(\frac{1}{\theta+\bar{\theta}_1} + \frac{\theta}{\theta\bar{\theta}_1 - R^2}\right) \qquad (A3.11)$$

$$\frac{\partial w_{cf}}{\partial k} = -\imath \ln \left(\frac{(\theta-\theta_1)}{(\theta+\bar{\theta}_1)} \frac{(\theta\theta_1 + R^2)}{(\theta\bar{\theta}_1 - R^2)}\right) \qquad (A3.12)$$

$$\frac{\partial w_{cf}}{\partial R} = \imath \frac{2RU_\infty \alpha}{\theta} - 2\imath k R \left(\frac{1}{\theta\theta_1 + R^2} + \frac{1}{\theta\theta_1 - R^2}\right) \qquad (A3.13)$$

$$\frac{\partial w_{s1}}{\partial b} = U_\infty \varepsilon \ln \theta \qquad (A3.14)$$

Finally, from equation (4) we have :

$$\frac{d\theta}{da} = \frac{d\theta}{dc}\frac{dc}{da} = -\frac{c^2}{2a\sqrt{\sigma^2 - c^2}} \qquad (A3.15)$$

$$\frac{d\theta}{d\sigma} = \frac{1}{2}\left(1 + \frac{\sigma}{\sqrt{\sigma^2 - c^2}}\right) \qquad (A3.16)$$

APPENDIX 4 : Program Listings

This appendix contains four FORTRAN programs :

The first one, ELLI, solves for the position of the vortex σ_1 from equations (27) and (30).

The second one, TRAVEL, computes the transformed velocity on the surface of the wing from equation (31).

The third one, CPELL, computes the pressure coefficient on the surface of the wing from equation (33).

Finally the fourth one, CLELL, computes the lift coefficient from equation (46).

```
      PROGRAM ELLI
C     ------------------------------------------------------------
C     THIS PROGRAM IS A NEWTON-RAPHSON ALGORITHM
C     IN TWO-DIMENSIONS (Y,Z).
C     THE FUNCTION F(S) WHOSE ROOTS ARE SEEKED IS COMPLEX.
C     THEREFORE, BOTH THE VARIABLE AND THE FUNCTION HAVE TO
C     BE SPLIT IN REAL AND IMAGINARY PARTS BEFORE THE
C     NEWTON-RAPHSON ALGORITHM CAN BE APPLIED.
C     THIS IS ACOMPLISHED BY THE SUBROUTINE "SPLIT".
C     ------------------------------------------------------------
      REAL J
      DIMENSION J(2,2)
C     ------------------------------------------------------------
C     INITIAL GUESS
C     ------------------------------------------------------------
      Y=?
      Z=?
C     ------------------------------------------------------------
   10 WRITE(5,100)Y,Z
  100 FORMAT(2E30.5)
      CALL JACOB(Y,Z,J)
      CALL SPLIT(Y,Z,F1,F2)
      DET=J(1,1)*J(2,2)-J(1,2)*J(2,1)
      HY=(J(2,2)*F1-J(1,2)*F2)/DET
      HZ=(J(1,1)*F2-J(2,1)*F1)/DET
      Y=Y-HY
      Z=Z-HZ
      IF(ABS(HY).LT.1.E-5.AND.ABS(HZ).LT.1.E-5) GO TO 20
      GO TO 10
   20 WRITE(5,100)Y,Z
      STOP
      END


      SUBROUTINE SPLIT(Y,Z,W1,W2)
      EXTERNAL F
      COMPLEX S,W,F
      S=Y+(0,1)*Z
      W=F(S)
      W1=REAL(W)
      W2=AIMAG(W)
      RETURN
      END


      SUBROUTINE JACOB(Y,Z,J)
      REAL J
      DIMENSION J(2,2)
      CALL SPLIT(Y,Z,F1,F2)
      DY=0.001
      Y1=Y+DY
      CALL SPLIT(Y1,Z,F1Y,F2Y)
      J(1,1)=(F1Y-F1)/DY
      J(2,1)=(F2Y-F2)/DY
      DZ=0.001
      Z1=Z+DZ
      CALL SPLIT(Y,Z1,F1Z,F2Z)
      J(1,2)=(F1Z-F1)/DZ
      J(2,2)=(F2Z-F2)/DZ
      RETURN
```

```
      END


      COMPLEX FUNCTION F(S)
      COMPLEX S,G1,G2,T,THO,TH1,QK1,QK2,QK,F1,F2,F3,F4,F5
C     ------------------------------------------------------------
C     DATA
C     ------------------------------------------------------------
      AE=?
      A=1.0
      B=?
      DY=?
C     ------------------------------------------------------------
      C=SQRT(A**2-B**2)
      R=0.5*(A+B)
C     ------------------------------------------------------------
C     If the separation point is on the upper surface DZ>0
C     If the separation point is on the lower surface DZ<0
C     ------------------------------------------------------------
      DZ=(+ or - )SQRT(B**2-B**2*(A-DY)**2/A**2)
      G1=CSQRT(S**2-C**2)
      G2=CONJG(G1)
      T=(A-DY+(0,1)*DZ+CSQRT((A-DY)**2-DZ**2-C*C+2*(0,1)*(A-DY)*DZ))/2
      THO=(S+G1)/2
      TH1=CONJG(THO)
      QK1=(TH1**2+2*T*TH1-R**2)/((T+TH1)*(T*TH1-R**2))
      QK2=(R**2+2*T*THO-THO**2)/((T-THO)*(T*THO+R**2))
      QK=(QK1-QK2)*T**2/(T**2+R**2)
      F1=(2*CONJG(S)+DY+(0,1)*DZ-A)/(A*AE)
      F2=(0,1)*(1+S/G1)*(0.5+R**2/(2*THO**2))
      F3=THO/(2*THO**2+2*R*R)-TH1/(2*THO*TH1-2*R*R)-1/(2*(THO+TH1))
      F4=(0,1)*C*C/(4*G1**2*THO)
      F5=B/(AE*G1)
      F=QK*(F1+F2-F5)+(0,1)*(1+S/G1)*F3-F4
      RETURN
      END
```

```
      PROGRAM TRAVEL
C     ------------------------------------------------------------
C     THIS PROGRAM COMPUTES THE TRANSFORMED VELOCITY
C     ON THE SURFACE OF A DELTA WING
C     WITH ELLIPTICAL CROSS-SECTION
C     EXHIBITING LEADING-EDGE SEPARATION
C     BY USING EQUATION (31) OF THE TEXT
C     ------------------------------------------------------------
      COMPLEX S,S1,S2,G,G1,G2,T,T1,T2,SP1,SP
      COMPLEX TA,T1A,T2A,TS,WT,WT1,WT2,WR,WB,WA
      COMPLEX Q,Q1,Q2,QF,QA,VCF,CV1,CV2,CV3,CV4
C     ------------------------------------------------------------
C     DATA
C     ------------------------------------------------------------
      A=1.0
      B=?
      ALFA=?
      AE=?
      DY=?
      S1=(?,?)
      GP=3.14159
C     ------------------------------------------------------------
      C=SQRT(A**2-B**2)
      R=(A+B)/2
      ALF=ALFA*3.14159/180.0
C     ------------------------------------------------------------
C     If the separation point is on the upper surface DZ>0
C     If the separation point is on the lower surface DZ<0
C     ------------------------------------------------------------
      DZ=(+ or -)(B/A)*SQRT(DY*(2*A-DY))
      X=(A*AE)/ALF
      Y=0.0
C     ------------------------------------------------------------
C     The "plus" sign is used for points on the upper surface
C     The "minus" sign is used for points on the lower surface
C     ------------------------------------------------------------
1     Z=(+ or -)B*SQRT(1-(Y/A)**2)
      S=Y+(0,1)*Z
      S2=CONJG(S1)
      G=CSQRT(S**2-C**2)
      G1=CSQRT(S1**2-C**2)
      G2=CSQRT(S2**2-C**2)
      T=(S+G)/2
      T1=(S1+G1)/2
      T2=(S2+G2)/2
      SP1=CSQRT((A-DY)**2+2*DZ*(A-DY)*(0,1)-DZ**2-C**2)
      SP=0.5*(A-DY+(0,1)*DZ+SP1)
      Q1=(SP+T2)*(SP-T1)*(SP*T2-R**2)*(SP*T1+R**2)
      Q2=SP**2*(T1+T2)*(R**2-T1*T2)
      Q=(Q1/Q2)*ALF
      QF=1/(T-T1)-1/(T+T2)+T1/(T*T1+R**2)-T2/(T*T2-R**2)
C     ------------------------------------------------------------
      TA=-C**2/(2*A*G)
      T1A=T1/A
      T2A=T2/A
      RA=R/A
      BA=B/A
      QA=Q/A
      TS=(1+S/G)/2
C     ------------------------------------------------------------
```

```
C       X - COMPONENT OF THE VELOCITY VECTOR
C       ------------------------------------------------------------
        WT=-(0,1)*ALF*(1+R**2/T**2)-(0,1)*Q*QF+B*(ALF/AE)/T
        WT1=(0,1)*Q*(1/(T-T1)-T/(T*T1+R**2))
        WT2=(0,1)*Q*(1/(T+T2)+T/(T*T2-R**2))
        CV1=CLOG(T-T1)
        CV2=CLOG(T+T2)
        CV3=CLOG(T*T1+R**2)
        CV4=CLOG(T*T2-R**2)
        IF(Y.LE.0.97)GO TO 2
        A1=AIMAG(CV1)+2*GP
        CV1=REAL(CV1)+(0,1)*A1
2       WQ=-(0,1)*(CV1-CV2+CV3-CV4)
        WRITE(5,100)Y,WQ
        WR=2*(0,1)*R*ALF/T-2*(0,1)*Q*R*(1/(T*T1+R**2)+1/(T*T2-R**2))
        WB=(ALF/AE)*CLOG(T)
C       ------------------------------------------------------------
        WA=WT*TA+WT1*T1A+WT2*T2A+WQ*QA+WR*RA+WB*BA
        VXS=(ALF/AE)*(B/X)*(ALOG(2*SQRT(X*(1-X)))-1/(2*(1-X)))
        VX=(ALF/AE)*REAL(WA)-VXS
C       ------------------------------------------------------------
C       CROSS FLOW VELOCITY COMPONENTS
C       ------------------------------------------------------------
        VCF=WT*TS
        VY=REAL(VCF)
        VZ=-AIMAG(VCF)
C       ------------------------------------------------------------
C       TRANSFORMED  VELOCITY
C       ------------------------------------------------------------
        TRAVEL=(AE*VY/ALF)-(Y/A)*(1+(ALF*VX/AE))
        WRITE(21,100)Y,TRAVEL
100     FORMAT(8F10.5)
        Y=Y+0.01
        IF(Y.LE.1.0)GO TO 1
        STOP
        END
```

```
      PROGRAM CPELL
C     ------------------------------------------------------------
C     THIS PROGRAM COMPUTES THE PRESSURE DISTRIBUTION
C     ON THE ELLIPTICAL CROSS-SECTION OF A DELTA WING
C     WITH SEPARATED FLOW
C     BY USING BERNOULLI'S EQUATION
C     ------------------------------------------------------------
      COMPLEX S,S1,S2,G,G1,G2,T,T1,T2,SP1,SP
      COMPLEX TA,T1A,T2A,TS,WT,WT1,WT2,WR,WB,WA
      COMPLEX Q,Q1,Q2,QF,QA,VCF,CV1,CV2,CV3,CV4
C     ------------------------------------------------------------
C     DATA
C     ------------------------------------------------------------
      A=1.0
      B=?
      ALFA=?
      AE=?
      DY=?
      S1=(?,?)
      GP=3.14159
C     ------------------------------------------------------------
      C=SQRT(A**2-B**2)
      R=(A+B)/2
      ALF=ALFA*3.14159/180.0
C     ------------------------------------------------------------
C     If the separation point is on the upper surface DZ>0
C     If the separation point is on the lower surface DZ<0
C     ------------------------------------------------------------
      DZ=(+ or -)(B/A)*SQRT(DY*(2*A-DY))
      X=(A*AE)/ALF
      Y=0.0
C     ------------------------------------------------------------
C     The "plus" sign is used for points on the upper surface
C     The "minus" sign is used for points on the lower surface
C     ------------------------------------------------------------
1     Z=(+ or -)B*SQRT(1-(Y/A)**2)
      S=Y+(0,1)*Z
      S2=CONJG(S1)
      G=CSQRT(S**2-C**2)
      G1=CSQRT(S1**2-C**2)
      G2=CSQRT(S2**2-C**2)
      T=(S+G)/2
      T1=(S1+G1)/2
      T2=(S2+G2)/2
      SP1=CSQRT((A-DY)**2+2*DZ*(A-DY)*(0,1)-DZ**2-C**2)
      SP=0.5*(A-DY+(0,1)*DZ+SP1)
      Q1=(SP+T2)*(SP-T1)*(SP*T2-R**2)*(SP*T1+R**2)
      Q2=SP**2*(T1+T2)*(R**2-T1*T2)
      Q=(Q1/Q2)*ALF
      QF=1/(T-T1)-1/(T+T2)+T1/(T*T1+R**2)-T2/(T*T2-R**2)
C     ------------------------------------------------------------
      TA=-C**2/(2*A*G)
      T1A=T1/A
      T2A=T2/A
      RA=R/A
      BA=B/A
      QA=Q/A
      TS=(1+S/G)/2
C     ------------------------------------------------------------
C     X - COMPONENT OF THE VELOCITY VECTOR
```

```
C       ------------------------------------------------------------
        WT=-(0,1)*ALF*(1+R**2/T**2)-(0,1)*Q*QF+B*(ALF/AE)/T
        WT1=(0,1)*Q*(1/(T-T1)-T/(T*T1+R**2))
        WT2=(0,1)*Q*(1/(T+T2)+T/(T*T2-R**2))
        CV1=CLOG(T-T1)
        CV2=CLOG(T+T2)
        CV3=CLOG(T*T1+R**2)
        CV4=CLOG(T*T2-R**2)
        IF(Y.LE.JUMP)GO TO 2
        A1=AIMAG(CV1)+2*GP
        CV1=REAL(CV1)+(0,1)*A1
2       WQ=-(0,1)*(CV1-CV2+CV3-CV4)
        WR=2*(0,1)*R*ALF/T-2*(0,1)*Q*R*(1/(T*T1+R**2)+1/(T*T2-R**2))
        WB=(ALF/AE)*CLOG(T)
C       ------------------------------------------------------------
        WA=WT*TA+WT1*T1A+WT2*T2A+WQ*QA+WR*RA+WB*BA
        VXS=(ALF/AE)*(B/X)*(ALOG(2*SQRT(X*(1-X)))-1/(2*(1-X)))
        VX=(ALF/AE)*REAL(WA)-VXS
C       ------------------------------------------------------------
C       CROSS FLOW VELOCITY COMPONENTS
C       ------------------------------------------------------------
        VCF=WT*TS
        VY=REAL(VCF)
        VZ=-AIMAG(VCF)
C       ------------------------------------------------------------
        CPSW=ALF**2-2*VX-VY**2-VZ**2
        WRITE(21,100)Y,CPSW
100     FORMAT(8F10.5)
        Y=Y+0.01
        IF(Y.LE.1.0)GO TO 1
        STOP
        END
```

```
      PROGRAM CLELL
C     ------------------------------------------------------------
C     THIS PROGRAM COMPUTES THE LIFT COEFFICIENT
C     FOR A DELTA WING WITH ELLIPTICAL CROSS-SECTION
C     EXHIBITING LEADING-EDGE SEPARATION
C     BY USING EQUATION (46) OF THE TEXT
C     ------------------------------------------------------------
      COMPLEX S,G1,G2,TH1,TH2,T,QK1,QK2,QK,FL
C     ------------------------------------------------------------
C     DATA
C     ------------------------------------------------------------
      OPEN(UNIT=6, FILE='TTY:',STATUS='NEW')
      A=1.0
      P=3.14159
1000  CONTINUE
      WRITE(5,10)
10    FORMAT(/,' Enter AE, S(complex), B,DY(real) below.')
      READ(6,*)  AE, S, B, DY
C     ------------------------------------------------------------
C     LINEAR PART OF LIFT
C     ------------------------------------------------------------
      CL1=2*P*AE
C     ------------------------------------------------------------
C     VORTEX LIFT
C     ------------------------------------------------------------
      C=SQRT(A**2-B**2)
      R=(A+B)/2
      G1=CSQRT(S**2-C**2)
      G2=CSQRT(CONJG(S)**2-C**2)
      TH1=S+G1
      TH2=CONJG(S)+G2
C     ------------------------------------------------------------
C     If the separation point is on the upper surface DZ>0
C     If the separation point is on the lower surface DZ<0
C     ------------------------------------------------------------
      DZ=(+ or -)B*SQRT(1-(A-DY)**2)
      T=(A-DY+(0,1)*DZ+CSQRT((A-DY)**2+2*(0,1)*(A-DY)*DZ-DZ**2-C*C))/2
      QK1=(.25*TH2**2+T*TH2-R**2)/((T+.5*TH2)*(.5*T*TH2-R**2))
      QK2=(R**2+T*TH1-.25*TH1**2)/((T-.5*TH1)*(.5*T*TH1+R**2))
      QK=T**2/(T**2+R**2)*(QK1-QK2)
      FL=(1+(A+B)/(A-B))*G1+(1-(A+B)/(A-B))*S
      CL2=(4*P*AE/(QK*A**2))*REAL(FL)
      CL=CL1+CL2
      WRITE(5,100)CL
100   FORMAT(/,F20.3)
      WRITE(5,200)
200   FORMAT(/,' Do you want to continue? (1 for yes- 0 for no) >',$)
      READ(6,*) ilog
      IF(ilog.EQ.1) GO TO 1000
      STOP
      END
```